EUROPEAN Journal of Molecular Biotechnology

Has been issued since 2013.
E-ISSN 2409-1332
2019. 7(1). Issued 2 times a year

Journal is indexed by: **Chemical Abstracts Service** (USA), **CiteFactor** – Directory of International Reseach Journals (Canada), **Cross Ref** (UK), **EBSCOhost Electronic Journals Service** (USA), **Global Impact Factor** (Australia), **Journal Index** (USA), **Electronic scientific library** (Russian Federation), **Open Academic Journals Index** (USA), **Sherpa Romeo** (Spain), **ULRICH's WEB** (USA).

All manuscripts are peer reviewed by experts in the respective field. Authors of the manuscripts bear responsibility for their content, credibility and reliability.

Editorial board doesn't expect the manuscripts' authors to always agree with its opinion.

Postal Address: 1367/4, Stara Vajnorska str., Bratislava – Nove Mesto, Slovakia, 831 04

Website: http://ejournal8.com/
E-mail: aphr.sro@gmail.com

Founder and Editor: Academic Publishing House Researcher s.r.o.

Release date 15.06.19
Format 21 × 29,7/4.

Headset Georgia.

Order № 19.

European Journal of Molecular Biotechnology

2019

Is. 1

CONTENTS

Articles and Statements

Published in the Slovak Republic
European Journal of Molecular Biotechnology
Has been issued since 2013.
E-ISSN: 2409-1332
2019, 7(1): 3-7

DOI: 10.13187/ejmb.2019.1.3
www.ejournal8.com

Articles and Statements

Complementation and Recombination Tests between Phage T4brii-1272 Mutant and Related Wild-Type Zonne Phages

Magda D. Davitashvili [a, *], Gela S. Azikuri [a]

[a] Iakob Gogebashvili Telavi State University, Georgia

Abstract

The investigation is concerned with the detection of the rII region in the phages, related to T-even, by means of some complementation and recombination tests with deletion mutant of phage T4BrII-1272. The restoration of the damaged function and the recombinants were detected by planting the progeny of reference and mutant strains of bacteria.

The analysis of the results obtained shows the ability of five phages out of the eight to restore the damaged function in deletion mutant of phage T4BrII-1272 (Zonne 2, Zonne 3 and Zonne 4 phages were not complement). The formation of recombinants was noted only with DDVI and Zonne 7 phages. The percentage of recombinants was 0.004 and 0.2 respectively.

Keywords: bacteriophages, recombinant phages, cistron, complementation, deletion mutant, phage T4BrII-1272, incubation efficiency, lysogenic, serological properties.

1. Introduction

To establish a genetic relationship between T-even phages, recombination analysis of population was successfully applied, which was generated by infecting common host cells (Hartl, Jones, 1998; Bohmer et al., 2010; Weaver, 2011; Kurtboke, 2012). It is noteworthy that recombinant phages may possess both parental properties, but it is not always possible to introduce the genes of one of the phages into the given genome (Laszlo et al., 2013). With the recombination, defined a degree of nonhomologous genes of T6 type phage groups was identified. They were separated from their natural habitats because they could not breed.

While working with a set of bacteriophages, it is difficult to prove, whether there are commonly identified properties for all bacterial infections in nature, or these qualities only characterize a definite group of phages.

The analysis of Benzer's complementation test (Benzer, 1957) with rII regions of the T4 phage helped to identify 2 cistrons (A and B) of this virus. In addition, the wild-type phage could restore both cistron's damaged functions.

Studies have shown (Chanishvili i dr., 1975) that both T4 phage and DDVI phage have rII-region (region/locus), which is also composed of 2 cistrons. A relatively simple method to identify the existence of rII regions in phages related to T–even phages can be a complemeting test of wild-type phages with T4BrII-1272 deletion mutant, which does not have both cistrons.

* Corresponding author
E-mail addresses: magdadav@gmail.com (M.D. Davitashvili)

The goal of the research was to detect rII regions with the complementation method in T-even phage-related wild-type zonne phages and with recombination testing of deletion mutant of phage T4BrII-1272.

2. Materials and methods

Bacteriophages: T2 and T4BrII-1272 Mutant phages, DDVI phage, Zonne 2 and Zonne 7 phages. Bacteria: *E. coli* B and *Sh. sonnei* 1188 strains were used to determine titers of phages, for crossbreeding and the analysis of the total number of progeny: E. coli B – with high titers in the complementation tests. Mutant clones – B / 2, B / 4, B / VI, II88 / 2, II88 / 4, II88 / VI, II88 / Zonne 2 – Zonne 7, K / 2, K / 4, K / VI, K // Zonne 2 – Zonne 7 – We used to analyze the progeny and calculate the share of the recombinants.

The quantitative complementation method is adopted from Jazikov et al. (Zhazykov i dr., 1970; Metody obshchei bakteriologii, 1984; Toth et al., 2013). The crossbreeding of phages was conducted in the following way: we added liquid culture of host bacterium to a mixture of two related phages. It was equally susceptible to both phages. The number of viable bacteria was determined with the photoelectric colorimeter. The infection rate equaled to 6 for every parental phage. After completing the time required for adsorption, we removed remained phage with a completely neutral dose of anti-phage serum, then we mixed the infected suspension with new broth and left at 30°C until the end of the lysis. The corresponding mixtures of lysate were incubated in etalon and mutant strains, allowing us to determine the production of parental and recombinant types of phages.

3. Results

We used the incubation method with indicator strains to determine the interdependence of different genotypes and populations (Harley, 2017). Table 1 presents the determining data of the effectiveness of bacterial viruses in etalon and mutant clones.

The presented material shows that all the clones of the phages are reproduced on *Sh. sonnei* 1188 and *E. coli* K-12 (λ) strains, the effectiveness of the incubation efficiency is insignificant (0,9-1,0). The exception is the T4BrII-1272 deletion mutant whose characteristic is only *E. coli* K-12 (λ phage lysogenic) adsorption properties on the strain without releasing the mature progeny. The efficiency of incubating bacteria in other sterile and mutant clones is 0,7-1,0. Phage Zonnes 2, 3, 4 are not reproduced on *E. coli* B (etalon and mutant) strains. Phage Zonne 5 is characterized by low efficiency in strains *E. coli* B and equals to 0,001.

Table 1. Comparative efficiency of phage incubation

Strains	Phages								
	T2	T4BrII-1272	DDVI	Zonne					
				2	3	4	5	6	7
E. coli B	1	1	1	-	-	-	0,001	1	1
E. coli K-12 (λ)	1	0	0,9	1	1	0,9	1	1	1
Sh. sonnei 1188	1	1	0,97	1	1	1	1	1	1
B/2	0	0	1	-	-	-	-	-	-
B/4	0	0	1	-	-	-	-	0,9	1
B/VI	0	0,9	0	-	-	-	-	-	-
1188/2	0	0	1	-	-	-	-	-	-
1188/4	0	0	1	0,8	0,95	-	-	0,9	0,9
1188/VI	-	1	0	-	-	-	-	-	-
1188/Zonne 2	-	1	-	0	0	0	0	-	-
1188/ Zonne 3	-	0,75	-	0	0	0	0	-	-

1188/ Zonne 4	-	1	-	0	0	0	0	-	-
1188/ Zonne 5	-	1	-	0	0	0	0	-	-
1188/ Zonne 6	-	0,75	-	-	-	-	-	0	-
1188/ Zonne 7	-	1	-	-	-	-	-	-	0
K/2	0	0	-	-	-	-	-	-	-
K/4	0	0	0	-	-	-	-	-	-
K/VI	-	0	0	-	-	-	-	-	-
K/ Zonne 2	-	0	-	0	0	0	0	-	-
K/ Zonne 3	-	0	-	0	0	0	0	-	-
K/ Zonne 4	-	0	-	0	0	0	0	-	-
K/ Zonne 5	-	0	-	0	0	0	0	-	-
K/ Zonne 6	-	0	-	-	-	-	-	0	-
K/ Zonne 7	-	0	-	-	-	-	-	-	0

Comparative analysis of the obtained results enables us to conclude that the strain *E. coli* B can not be used as bacteria-host for all phages. On the basis of the above mentioned we have used *Sh. sonnei* 1188 clone. The results of the test are presented in Table 2.

Table 2. Quantitative complementation between phages

Phage experimental solution	**The phage production calculated on single infected bacteria**	
	Wild type	**T4BrII-1272**
T2 and T4BrII-1272	40	54
DDVI ও T4BrII-1272	100	52
Zonne 2 ও T4BrII-1272	10	0
Zonne 3 ও T4BrII-1272	17	0
Zonne 4 ও T4BrII-1272	18	0
Zonne 5 ও T4BrII-1272	46	11
Zonne 6 ও T4BrII-1272	86,9	129
Zonne 7 ও T4BrII-1272	60,6	75

Simultaneously infecting wild type and T4BrII-1272 deletion mutant phage of bacterial cells confirms that positive complementation was only in the following cases - T2 and T4BrII-1272 (control), DDVI and T4BrII-1272, Zonne 5 and T4BrII-1272, Zonne 6 and T4BrII- 1272, Zonne 7 and T4BrII-1272. This circumstance proves that the function of the rII region in T4 phage can be compensated by the region function of some wild-type phages. Complementation was not observed in the following cases – Zonne 2 and T4BrII-1272, Zonne 3 and T4BrII-1272, Zonne 4 and T4BrII-1272. It is also detected that some phages multiplied with deletion mutants (produce 10-18 particles in a cell).

A high range of phage mixture cross-breeding was conducted in Sh. sonnei 1188 cells by infecting; one of which was the T4BrII-1272 mutant, and the second- wild-type, and then analyzed the reproduction. We considered the particles as recombinants if they gave transparent negative colonies in reference to the wild type phages in *E. coli* K-12 sustainable mutant strain, as the genome of the recombinant phage should contain the locus which is responsible for rapid lysis – in a wild type of phage, and a locus responsible for the lysis spectrum – T4BrII-1272 phage. The results of the test are summarized in Table 3 with a mean value of 3-4 tests.

Table 3. Recombination between deletion Mutant T4BrII-1272 and wild type of zonne phage

Cross-breeded phages	Recombination, %
T2 and T4BrII-1272	0,12
DDVI and T4BrII-1272	0,004
Zonne 2 and T4BrII-1272	-
Zonne 3 and T4BrII-1272	-
Zonne 4 და T4BrII-1272	-
Zonne 5 და T4BrII-1272	-
Zonne 6 და T4BrII-1272	-
Zonne 7 და T4BrII-1272	0,2

The recombination between the phages was observed only in the following cases: T2 and T4BrII-1272 (control), DDVI and T4BrII-1272, Zonne 7 and T4BrII-1272. The percentage of the recombination rate was 0.004-0,12. Obtained recombinants were selected and incubated in a host strain and re-examined on the activity of lytic spectrum.

In other cases, crossbreeding was not observed. The low percentage of recombination between T2 and T4BrII-1272 phages may be attributed to characteristics of Sh. sonnei 1188 strain which was used for the tests, as the recombinant percentage of T2 and T4BrII-1272 increased up to 1,4 by the hybridization of these viruses in E. coli B strain.

Three types of reactions were revealed by quantitative complementing experimental analysis between T4BrII-1272 deletion mutant and morphologically identical and serologically relevant phage types:

1. T4BrII-1272 Function restoration in both phages during simultaneous reproduction (T2 and T4BrII-1272, DDVI and T4BrII-1272, Zonne 6 and T4BrII-1272, Zonne 7 and T4BrII-1272)
2. Function restoration of T4BrII-1272 during partial inhibition of its reproduction (Zonne 5 and T4BrII-1272);
3. No complementation (Zonne 2 and T4BrII-1272, Zonne 3 and T4BrII-1272, Zonne 4 and T4BrII-1272).

The system of phage incubation developed by us, after the compound infection of the cells, in the phage-resistant wild type *E. coli* K-12 (λ) mutant strains, in which the wild clone under the study in normal conditions is not adsorbed, and the deletion mutant is not producible, enabled us the possibility to discern quite rare recombinants, that bear rII region from the wild type phage, while h locus – from T4B phage. Taking into account the final solutions, we could propose even isolation of recombinant units. The use of this system is justified by the fact that none of the phages under the study had corresponding h locus of T4 phage, whereby resistant mutants were simultaneously exposed to lysis.

As the results of the studies have shown, only in case of cross-breeding of the following phages T2 and T4BrII-1272, DDVI and T4BrII-1272, Zonne 7 and T4BrII-1272, recombinants were produced, whose stability was established in the next generations. The frequency of appearance of recombinant, as well as in the case of T-even crossbreeding, depends on the binding quality of genes. The greater the distance between the genes, the greater the likelihood of cross-binding between them and the higher the share of recombinant generations.

4. Conclusion

The study of the correlation between the restoration of function and recombination between viruses used in the tests shows that when the phage can restore the damaged function of the rII region, not in all cases cross-breeding is possible. It is not always possible to establish complementation, recombination, and relationship between biological signs (capsid's structure, serological properties, etc.).

Thus, three types of reactions identified between selected 8 phages and the genomes of T4BrII-1272 deletion mutant indicate the existence of different degrees of relations between these bacterial viruses that were developed due to evolution.

References

Benzer, 1957 – *Benzer S.* (1957). The Chemical Basis of Heredity (eds. W. D. Elroy and B. Glass). Johns Hopkins Press. Baltimore.

Bohmer et al., 2010 – *Bohmer D., Repiska V., Danisovic L.* (2010). Introduction to medical and molecular biology. Bratislava: Asklepios.

Chanishvili i dr., 1975 – *Chanishvili, T. G., Kapanadze, Zh. S., Alavidze, M.A.* (1975). *Izv. AN GSSR, ser. Biol.,* I, 1, 78-86. [in Russian]

Harley, 2017 – *Harley, J.* (2017). Laboratory Exercises in Microbiology. 10th edition. McGraw-Hill Publishing.

Hartl, Jones, 1998 - *Hartl D.L., Jones E.W.* (1998). Genetics:Principles and Analysis. Fourth Edition. Jones and Bartlett Publishers.

Kurtboke, 2012 – *Kurtboke I.* (2012). Bacteriophages. In Tech, Croatia.

Laszlo et al., 2013 – *Laszlo V., Toth S., Pap E., Szalai C., Falus A., Oberfrank F.* (2013). Genetics and Genomics. Budapest University of Technology and Economics. Typotex Kiado.

Metody obshchei bakteriologii, 1984 – Metody obshchei bakteriologii [Methods of general bacteriology]. T. 3, M.: «MIR», 1984. [in Russian]

Toth et al., 2013 – *Toth, E.M., Borsodi, A.K., Felfoldi, T., Vajna, B., Sipos, R. and Marialigeti, K.* (2013). Practical Microbiology.Eotvos Lorand University.

Weaver, 2011 – *Weaver, R.F.* (2011). Molecular Biology. 5th edition. University of Kansas. Quad/Graphics.

Zhazykov i dr., 1970 – *Zhazykov I., Krylov V.N., Alikhanyan S.I.* (1970). Genetika [Genetics]. VI, 8, 135-138. [in Russian]

Published in the Slovak Republic
European Journal of Molecular Biotechnology
Has been issued since 2013.
E-ISSN: 2409-1332
2019, 7(1): 8-16

DOI: 10.13187/ejmb.2019.1.8
www.ejournal8.com

Regioselectivite and Reactivity of the Pyridinein Nucleophilic Substitution Reaction: DFT Study

M. El idrissi [a, *]

[a] Chouaïb Doukkali University, El Jadida, Morocco

Abstract

In this work, we theoretically studied the regioselectivity experimentally observed in the substitution reactions between pyridine and nucleophile (KOH, $NaNH_2$ and EtMgX). This work was done using the DFT method at the B3LYP/6-31G (d) level. The analysis of the OMF, ESP and the reactivity indices derived from the DFT confirm the regioisomeric path of these reactions. The analysis of the energies of the products shows that these substitution reactions favor the regioselectivity, moreover we examined the pyridine like catalyst in the reaction alcylation, and our study shows that pyridine is a good catalyst for esterification reactions. The results obtained are in agreement with the experimental data.

Keywords: Density Functional Theory, Pyridine, Becke 3-Parameter Lee-Yang-Parr, Frontier Molecular Orbital, The global DFT indices, Parr functions.

1. Introduction

The chemistry of heterocyclic products is one of the most complex branches of organic chemistry (Boukis et al., 2017). It is evenly exciting for, its theoretical proposition, for the variety of its synthetic procedures, and for the pharmacological and industrial connotation of heterocyclic products (Arrieta et al., 2007; Aucagne et al., 2007; Wang et al., 2012; Zaki et al., 2017). A field of such importance and essential complexity should be made as gladly accessible as possible, and to be short of a current detailed and comprehensive presentation of heterocyclic chemistry is so fervently felt. It is the aim of the present series to fill this gap by specialist presentations of variety branches of heterocyclic chemistry. Pyridine is a limpid, slightly yellowish liquid with an unpleasant and penetrating odor (sour, putrid and fish-like). Pyridine derivatives such as Vitamin B3, Vitamin B6 (Figure 1) and pyridoxal phosphate which is an essential coenzyme in a significant number of amino acid reactions (transaminations, decarboxylations and racemisations).

* Corresponding author
E-mail addresses: idrissi_82@hotmail.fr (M. El idrissi)

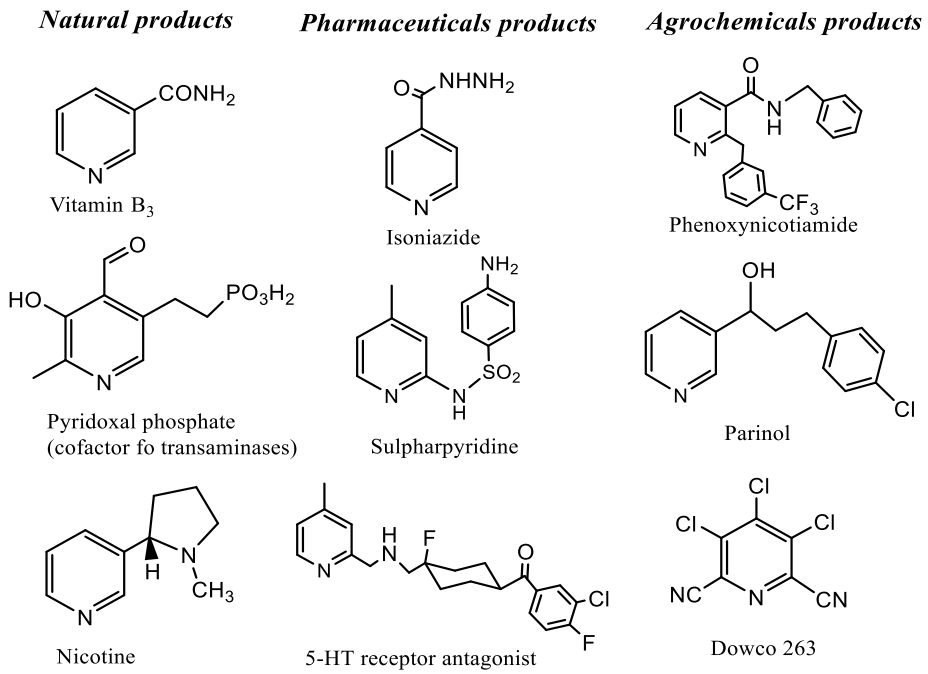

Fig. 1. Pyridine and pyridine derivatives

Pyridines (or azines) are organic compounds widely used in agrochemicals and pharmaceuticals (Davis et al., 2005). Pyridines are used to make drugs, insecticides, herbicides, dyes, paints, disinfectants and explosives. Pyridines also have the function of a catalyst in certain chemical reactions such as condensation or halogenation (introduction of halogen atoms in a reaction) (Corma, 1995). Pyridine is also widely used as an organic solvent; it is also used to denature the commercial ethanol used for the same purpose. It is also used in the manufacture of many pharmaceutical products, rubber and as a waterproofing, bactericidal and insecticide.

Pyridine is prepared by the method of synthesis of Hantzsch (Hantzsch, 1981; Henry, 2004), that is a reaction between an aldehyde, with two equivalents of β-keto ester and a nitrogen donor makes it possible to obtain a dihydropyridine which by oxidation (by HNO3, Ce (IV) or a quinone), the solvent utulized may be water or ethanol (Figure 3). Pyridines can be extracted from bone tars (Dippel animal oils) by the action of dilute sulfuric acid. After evaporation, it is taken up with sodium hydroxide and distilled.

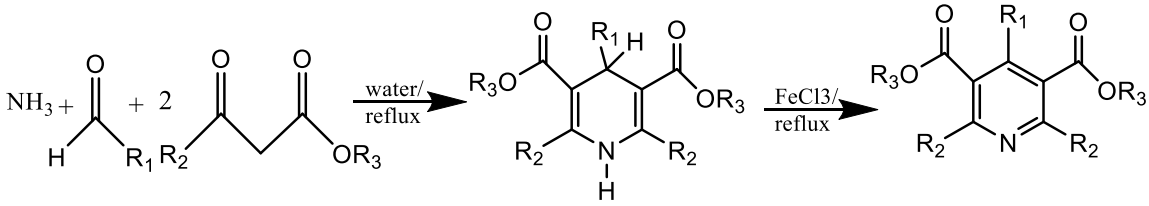

Fig. 2. The method of synthesis of Hantzsch

Our aim in this work is to present a theoretical study of substitution reactions of the pyridine and compared the results of our computations with experimental outcomes obtainable in the literature.

2. Computational methods

DFT computations were carried out using the B3LYP functional (Yanai et al., 2004), together with the standard 6-31(d) basis set (Yanai et al., 1982). The optimizations have been realized using the Berny analytical gradient optimization method. All computations have been shown with the Gaussian 09 suite of programs (Frisch et al., 2009). The global electrophilicity index (Parr et al., 2009) ω, was given by the following expression $\omega = \frac{\mu^2}{2\eta}$, in terms of the electronic chemical

potential μ and the chemical hardness η. Both quantities could be approached in terms of the one-electron energies of the frontier molecular orbital HOMO and LUMO, ε_H and ε_L as $\mu = \frac{\varepsilon_H + \varepsilon_L}{2}$ and $\eta = \varepsilon_H - \varepsilon_L$, respectively. The empirical nucleophilicity index N (Domingo et al., 2008; Domingo, Pérez 2011), based on the HOMO energies obtained within the Kohn-Sham (Kohn, Sham, 1965), and defined as $N = E_{HOMO}(Nu) - E_{HOMO}(TCE)$. the nucleophilicity was referred to tetracyanoethylene (TCE). This choise allowed us to handle conveniently a nucleophilicity scale of positive values. Electrophylic P_k^+ and nucleophilic P_k^- Par functions were obtained through analysis of the Mulliken atomic spin density (ASD) of the radical anion and radical cation of the reagents. The local electrophilicity and the local nucleophilicity indices were evaluated using the following expressions $\omega_k = \omega P_k^+$ and $N_k = NP_k^-$ (Ourhriss et al., 2018; El Haib et al., 2018; Ourhriss et al., 2017; El Idrissi et al., 2017; Zeroual et al., 2017a; Zeroual et al., 2017b; Zeroual et al., 2017c; Zeroual et al., 2017d; Zoubir et al., 2017a; Zoubir et al., 2017b; Zoubir et al., 2017c; Zeroual et al., 2017; Zeroual et al., 2017; El Idrissi et al., 2017; Zoubir et al., 2016; Zeroual et al., 2016; El Idrissi et al., 2016; Zeroual et al., 2015a; Zeroual et al., 2015b; Zeroual et al., 2015c; Zeroual et al., 2015d; Zeroual et al., 2015e; Zeroual et al., 2015f; Zeroual et al., 2015g; Zeroual et al., 2015h; Barhoumi et al., 2015; Ryachi et al., 2015; Zeroual et al., 2014a; ; Zeroual et al., 2014b; ; Zeroual et al., 2014c; El Idrissi et al., 2013). The stationary points were characterized by frequency computations in order to verify that TSs have one and only one imaginary frequency. Intrinsic reaction coordinate (IRC) (Fukui, 1970) pathways were traced to verify the connectivity between minima and associated TSs.

3. Results and discussion

The current theoretical study has been divided in seven parts: (1) an examination of the conceptual DFT indices of the reagents involved in electrophilic and nucleophilic substitution reaction of pyridine with KOH, NaNH2 and dichloromethane. (2) Next, the investigation of the HOMO, LUMO and ESP of the reagents. (3) Then, thermodynamic examination of these reactions to understand the regiolelectivity observed. (4) After that, the theoretical study of reaction between pyridine and EtMgX, (5) Moreover, scrutinizing a pyridine as a catalyst in acylation reactions, (6) in addition, the theoretical study of aromatic electrophilic substitution of pyridine. (7) Finally, Thermodynamic study of the eletrophilic substitution reaction of pyridin-2-amine.

3.1 The conceptual DFT indices of the reagents involved in substitution reaction of pyridine with KOH and NaNH2

The global DFT indices, namely the electronic chemical potential μ, chemical hadness η, electrophilicity w and nucleophilicity N, are given in Table 1.

Table 1. B3LYP/6-31G(d) chemical hardness, electronic chemical potential, electrophilicity, nucleophilicity in eV, of the pyridine, KOH and NaNH2 there total energies

	η	μ	ω	N	ΔNmax	Energy
Pyridine	6.26	-3.74	1.11	2.65	0.59	-248.284973
KOH	2.42	-2.54	1.33	5.77	1.04	-675.7130626
$NaNH_2$	2.29	-2.76	1.67	5.61	1.20	- 218.2212268

The electronic chemical potential of pyridine, −3.74 eV, is higher than that of acetic dichloromethane, −4.43 eV, indicating that along a polar reaction the global electron density transfer (GEDT) will flux from the pyridine framework towards the dichloromethane. The electrophilicity ω and nucleophilicity N indices of the simplest pyridine are 1.11 and 2.65 eV, being classified on the borderline of marginal electrophiles and as a strong nucleophile within the electrophilicity and nucleophilicity scales. On the other hand, dichloromethane has a global electrophilicity ω index of 1.22 eV and a nucleophilicity N index of 1.10 eV, being classified as a strong electrophile and as a marginal nucleophile.

Consequently, it is expected that the , dichloromethane participates as a good electrophile towards the strong nucleophilic pyridine.

Other hand the electronic chemical potential of KOH and $NaNH_2$, −2.42, -2.76 eV, are higher than that of pyridine, −3.74 eV, indicating that along a polar reaction the global electron density transfer) will flux from the KOH and $NaNH_2$ framework towards the pyridine. The electrophilicity ω and nucleophilicity N indices of the simplest KOH and $NaNH_2$ are 1.33, 1.67 and 5.77, 5.61 eV, being classified on the borderline of marginal electrophiles and as a strong nucleophile within the electrophilicity and nucleophilicity scales.

Consequently, it is expected that the , pyridine participates as a good electrophile towards the strong nucleophilic KOH and $NaNH_2$.

3.2 The analyze of the HOMO, LUMO and ESP of the reagents

As the non-symmetric reagents, the preliminary two-center interaction involving the most electrophilic center of the electrophile and the most nucleophilic center of the nucleophile.

To pinpoint the actives regions of these reagents, we have illustrated in Figure 3 the density of the HOMO, LUMO orbital and ESP of the reagents.

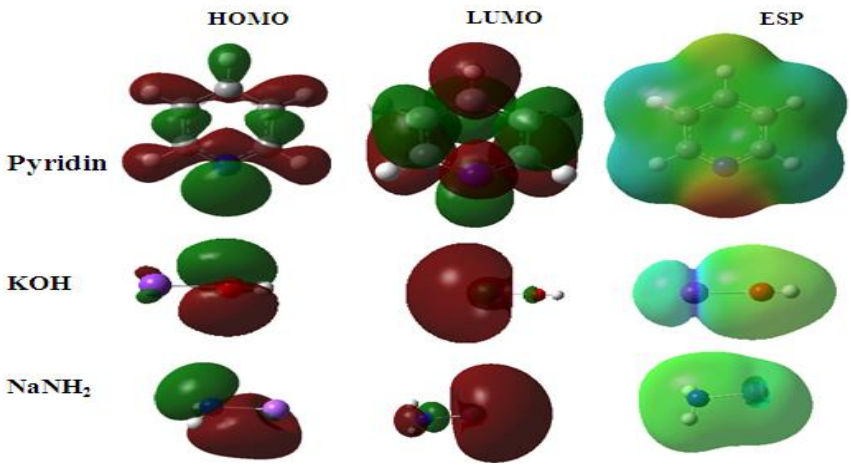

Fig. 3. The density of the HOMO, LUMO orbital and ESP of the reagents

According to the density of the HOMO orbital of the reagents, we find that the HOMO orbital is located on the nitrogen atom and para carbon atom of pyridine, for the KOH, NaNH2 and DCM molecules is located respectively on the oxygen atom, the nitrogen atom and the atom of chlorine. This result is confirmed by EPS these centers possess a red color what to indicate that these centers carry a negative charge.

3.3 Thermodynamic Study of the substitution reaction of pyridine with KOH and NaNH2

Due to the asymmetry of the pyridine, the substitutions reactions between pyridine and nucleophiles (KOH and NaOH) can take place along three regioisomeric pathways, the ortho, the meta and para, leading to the formation of the 1a, 2a, 3a, 1b, 2b and 3b, respectively (Figure 4).

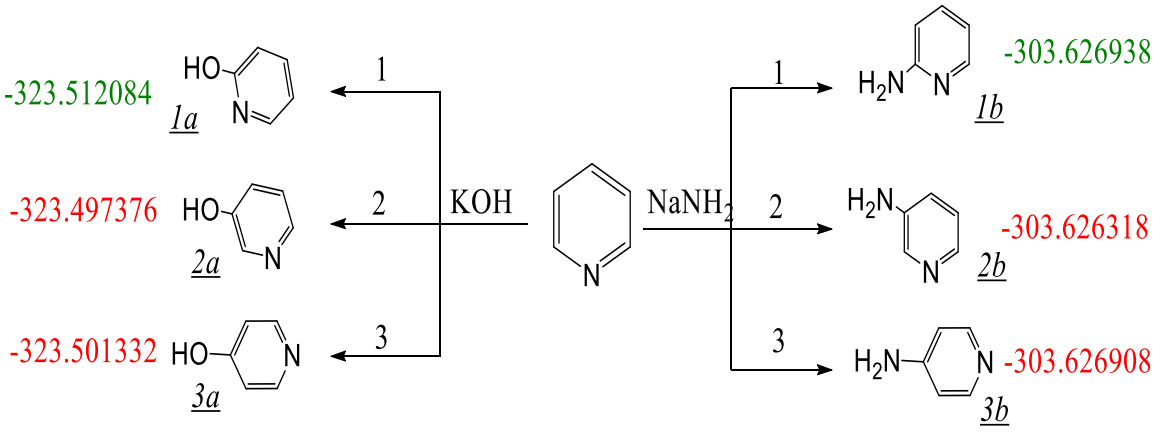

Fig. 4. Studied competitive regioisomeric channels associated with the substitutions reactions between pyridine and nucleophiles (KOH and NaOH). (energies in Atomic Unit)

The gas phase formations of the products 1a, 2a, 3a, 1b, 2b and 3b are: -323.512084 (1a), -323.497376 (2a), -323.501332 (3a) -303.626938 (1b), -303.626318 (2b) and -303.626908 (3b) A.U. The conclusion can be drawn from these energy results, the formation of the products 1a and 1b are favored in good agreement.

3.4 Understanding the regioselectivity in reaction between pyridine and EtMgX

Electrophilic aromatic substitutions are difficult to realize because pyridine is less reactive than benzene. In this part we study the reaction between pyridine and acetyl chloride, after that we study the reaction between the product obtained and EtMgCl to examine the regioselectivity experimentally observed. In Figure 5, we show the reaction paths and the energies of the products obtained by the method DFT/6-31 (d).

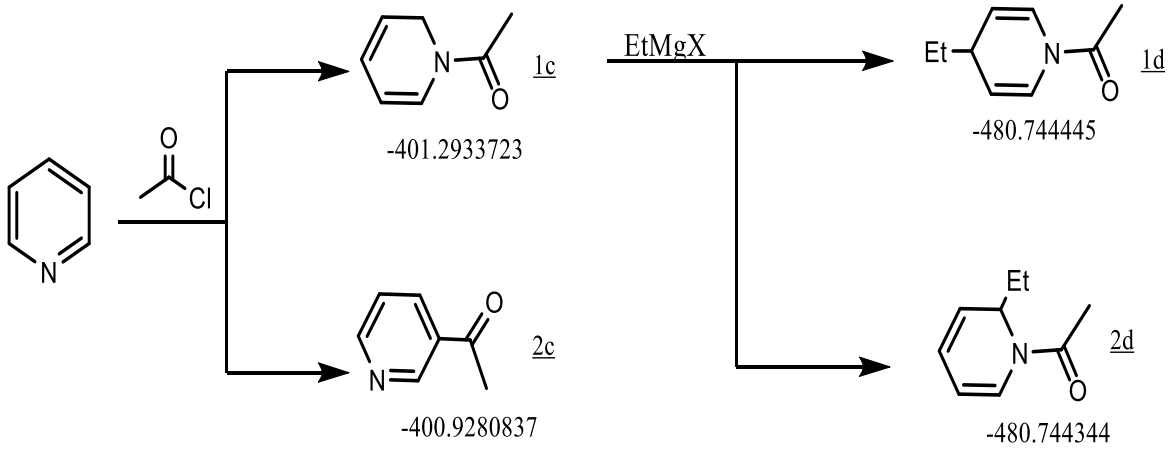

Fig. 5. Studied competitive regioisomeric channels associated with the substitutions reactions of pyridine (energies in Atomic Unit)

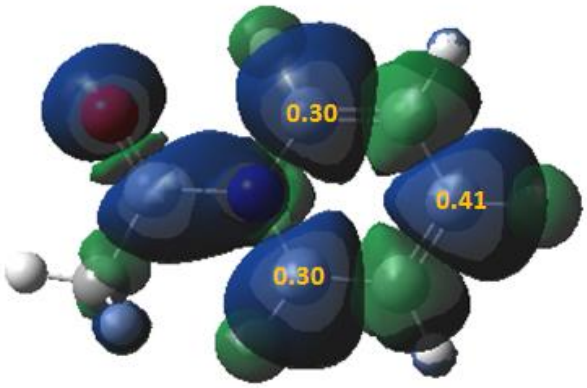

Fig. 6. 3D representations of the ASD of the radical cation the electrophilic P_k^+ Parr functions 1-acetylpyridin-1-ium

The energy of the product 1c. (-401.2933723) is lower than the product energy 2c (-400.9280837), which shows that the product 1c is thermodynamically favorable, moreover the energy of the product 1d is (-480.744445) is lower than the energyof the product 2d (-481.744344) which shows that the product 2d is thermodynamically favorable. In Figure 7 we have illustrated the electrophilic functions of Parr of the product 1c, according to this figure we find that the value of electrophilic functions of Parr in the carbon atom 4 is greater than the value at the carbon atom 1, which confirms that the nucleophilic attack is favorable in the carbon 4.

3.5 Pyridine as a catalyst in acylation reactions

The central principle of catalysis lies in the fact that the active sites are indeed involved in the intermediate stages of the reaction, but that they are regenerated at the end of the process, thus

recovering their initial characteristics, the catalyst is therefore not consumed during the reaction: it can thus be used in limited quantities and act efficiently for long periods without the need for replacement. In this section, we examined the effect of pyridine as catalysts on the esterification reaction between methanol and Acetyl chloride.

We have reassembled in Table 2 the energy of the HOMO, LUMO orbital and the energy gap between the two frontiers orbital of the methanol, acetyl chloride and acetyl chloride with pyridine, and in Figure 7 we have illustrated the maps of the HOMO, LUMO orbital and the energy gap between the two orbital.

Table 2 B3LYP/6-311G(d) the energy of the HOMO, LUMO orbital and the energy gap between the two frontiers orbital of the two partners

	Methanol	Acetyl chloride	Acetyl chloride + pyridine
HOMO	-7.19	-8.16	-2.16
LUMO	2.04	-1.13	-6.18
$\lvert E^{HOMO}_{Methanol} - E^{LUMO}_{Acetyl} \rvert$	-------	6.06	5.03
$\lvert E^{LUMO}_{Methanol} - E^{HOMO}_{Acetyl} \rvert$	-------	10.20	8.22

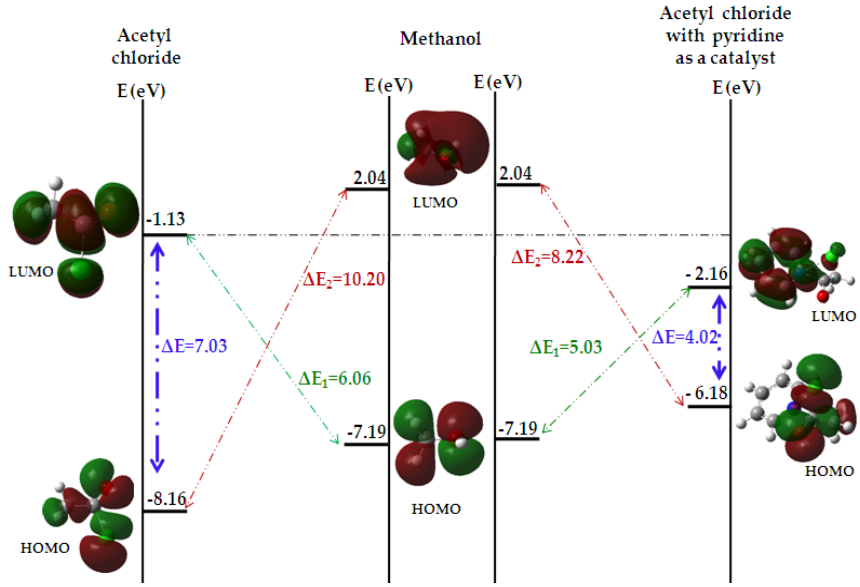

Fig. 7. 3D representations of the HOMO, LUMO of methanol acetyl chloride and acetyl chloride with pyridine

We note from Table 2 and Figure 7 that the energy gap between the HOMO and LUMO orbital of the reagents without pyridine as a catalyst is of order: ΔE_1 = 6.06, ΔE_2 = 1.20 and ΔE = 7.03. When pyridine is used as a catalyst, the difference becomes of order: .E_1 = 5.03, ΔE_2 = 8.22 and ΔE = 4.02. Therefore the presence of pyridine as a catalyst promotes esterification reactions in good agreement with experimental observations.

4. Conclusion

In this chapter, we have discussed the regioselectivity of the substitution reactions between pyridine and KOH, NaNH2 and EtMgX, this work was done using within Density Functional Theory at the B3LYP / 6-31G (d) level. Analysis of the conceptual DFT indices indicates that these reactions are highly regioselective, in addition our study shows that pyridine is a good catalyst for esterification reactions.

5. Conflict of Interest

The authors declare that there is no conflict of interests regarding the publication of this paper. Also, they declare that this paper or part of it has not been published elsewhere.

References

Arrieta et al., 2007 – *Arrieta A., Otaegui D., Zubia A., Cossío F.P., Díaz-Ortiz A., De la Hoz A., Herrero M. A., Prieto P., Foces-Foces C., Pizarro J.L., Arriortua, M.I.* (2007). Solvent-Free Thermal and Microwave-Assisted [3 + 2] Cycloadditions between Stabilized Azomethine Ylides and Nitrostyrenes. An Experimental and Theoretical Study, *J. Org. Chem*, 72, 4313-4322.

Aucagne et al., 2007 – *Aucagne V., Berna J., Crowley J.D., Goldup S.M., Hänni K.D., Leigh D.A., Lusby P.J., Ronaldson V.E., Slawin A. M.Z., Viterisi A., Walker D.B.,* (2007). Catalytic "Active-Metal" Template Synthesis of [2]Rotaxanes, [3]Rotaxanes, and Molecular Shuttles, and Some Observations on the Mechanism of the Cu(I)-Catalyzed Azide–Alkyne 1,3-Cycloaddition, *J. AM. CHEM. SOC.*, 129, 11950-11963.

Barhoumi et al., 2015 – *Barhoumi A., Zeroual A., Bakkas S., El Hajbi A.* (2015). Theoretical study of the regioselectivity of the reaction between tetrachloromethane and triethyl phosphite using the DFT B3LYP/6-31G (d) method." *Journal of Computational Methods in Molecular Design*, 5 (2), 8-15.

Boukis et al., 2017 – *Boukis A.C., Monney B., AR Meier M.,* (2017). Synthesis of structurally diverse 3,4-dihydropyrimidin-2(1H)-ones via sequential Biginelli and Passerini reactions. *Beilstein J Org Chem.*, 13, 54-62.

Corma, 1995 – *Corma A.* (1995). Inorganic Solid Acids and Their Use in Acid-Catalyzed Hydrocarbon Reactions. *Chem. Rev.*, 95 (3), 559-614.

Davis et al., 2005 – *Davis J.M., Truong A., Hamilton A.D.* (2005). Synthesis of a 2,3';6',3'' -Terpyridine Scaffold as an α-Helix Mimetic. *Org. Lett.,* 7 (24), 5405-5408.

Domingo 2014 – *Domingo L.R.* (2014). A new C–C bond formation model based on the quantum chemical topology of electron density. *RSC Adv,* 4: 32415-32428.

Domingo et al 2008 – *Domingo L.R., Chamorro E., Pérez P.* (2008). Understanding the Reactivity of Captodative Ethylenes in Polar Cycloaddition Reactions. A Theoretical Study. *J. Org. Chem*, 73: 4615-4624.

Domingo et al., 2016 – *Domingo L.R., Ríos-Gutiérrez M., Pérez P.* (2016). A new model for C–C bond formation processes derived from the Molecular Electron Density Theory in the study of the mechanism of [3+2] cycloaddition reactions of carbenoid nitrile ylides with electron-deficient ethylenes. *Tetrahedron,* 72: 1524-1532.

El Haib et al., 2018 – *El Haib A., Elajlaoui R., El Idrissi M., Moumou M., Abouricha S., Zeroual A., Benharref A., El Hajbi A.* (2018). The mechanism, the chemoselectivity and the regioselectivity of the 1-Benzyl-4-ethynyl-1H-[1,2,3]triazole and 1-Azidomethyl-4-tert-butyl-benzene in [3+2] cycloaddition reactions: a DFT study, *Mor. J. Chem.* 6(1), 14-21.

El Idrissi et al., 2013 – *El Idrissi M., Zeroual A., Benharref A., El Hajbi A.* (2013). Determination of certain thermodynamic and geometric values and condensation mechanism of β-himachalene and dibromocarbene using density functional theory (DFT), *Phys. Chem. News,* 69, 89-95.

El Idrissi et al., 2016 – *El Idrissi M., El Haib A., Zoubir M., Hammal R., Zeroual A., El Hajbi A.* (2016). Understanding the regioselectivite of the Baeyer-Villiger reaction of bicyclo[4.2.0]octan-7-one and bicyclo[3.2.0]heptan-6-one: A DFT Study. *Journal of Computational Methods in Molecular Design.*, 6 (3), 75-79.

El Idrissi et al., 2016 – *El Idrissi M., Zoubir M., Zeroual A., El Ajlaoui R., El Haib A., Benharref A., El Hajbi A.* (2016). A theoretical study of the mechanism and regioselectivity of the 1,3-dipolar cycloaddition reaction of azides with alkynes. *Journal Marocain de Chimie Hétérocyclique*, 15 (1), 146-151.

El Idrissi et al., 2017 – *El Idrissi M., El Ajlaoui R., Zoubir M., Abouricha S., Moumou M., Zeroual A., Benharref A., El Hajbi A.* (2017). Theoretical study of the chemo- and regioselectivity of the [3+2] cycloaddition reaction between mesitonitrile oxides and 2-fluoren-9-ylidene-malononitrile. *J. Mater. Environ. Sci.*, 8 (10), 3564-3569.

El Idrissi et al., 2017 – *El Idrissi M., Zeroual A., El Haib A., Benharref A., El Hajbi A.* (2017). Theoretical study of the mechanism and regioselectivity of electrophilic substitution reaction between the ar-himachalene and acetic anhydride. *International Journal of Multidisciplinary Sciences,* (2), 1-10.

El Idrissi et al., 2017 – *El Idrissi M., Zoubir M., Zeroual A.* (2017). Understanding the mechanism and regioselectivity of Prop-2-yn-1-ol with azido-compounds in [3+2] cycloaddition reactions: a molecular electron density theory study. *Journal Marocain de Chimie Hétérocyclique*, 16 (1), 179-185.

Francl et al., 1982 – *Francl M.M., Pietro W.J., Hehre W.J.* (1982). A polarization-type basis set for second-row elements. *J. Chem. Phys,* 77: 3654-3665.

Frisch et al., 2009 – Gaussian 09, Revision A.02, Frisch M. J. et al.

Fukui 1970 – *Fukui, K.* (1970). Formulation of the reaction coordinate. *J. Phys. Chem,* 74: 4161-4163.

Hantzsch, 1981 – *Hantzsch A.* (1981). Condensation produkte aus Aldehydammoniak und Ketoniartigen Verbindungen. Ber. 14, 1637-1638.

Henry, 2004 – *Henry G.D.* (2004). De novo synthesis of substituted pyridines, Tetrahedron,; 60: 6043-6061.

Ourhriss et al., 2017 – *Ourhriss N., Zeroual A., Ait ElHad M., Mazoir N., Abourriche A., Gadhi C.A., Benharref A., El Hajbi A.* (2017). Synthesis of 1-isopropyl-4,7-dimethyl-3-nitronaphthalene: An experimental and theoretical study of regiospecific nitration. *J. Mater. Environ. Sci.*, 8 (4), 1385-1390.

Ourhriss et al., 2017 – *Ourhriss N., Zeroual A., Gadhi C. A., Benharref A., Abourriche A., Bennamara A., El Hajbi A.* (2017). Synthesis, spectroscopic NMR and theoretical (HF and DFT) investigation of 3,5,5,9-tetramethyl-2-nitro-6,7,8,9-tetrahydro-5H-benzocycloheptene and 2,5,9,9-tetramethyl-1,3-dinitro-6,7,8,9-tetrahydro-5H-benzocycloheptene. *European Journal of Molecular Biotechnology*, 5(2), 52-59.

Ourhriss et al., 2018 – *Ourhriss N., Zeroual A., Gadhi C. A., Benharref A., Abourriche A., Bennamara A., El Hajbi A.* (2018). A Regioselective and Stereoselective Synthesis of 2,5-Dichloro-2,5,9,9-tetramethyl-decahydro-benzocycloheptene via Stepwise addition Reactions between α-himachalene and HCl: Experimental and Theoretical Study. *European Reviews of Chemical Research*, 5(1), 22-29.

Ryachi et al., 2015 – *Ryachi K., Zeroual A., Khamliche L., Bakkas S., El Hajbi A.* (2015). Understanding the regioselectivity and reactivity of some ethylene compounds using Parr functions. *J. Nat. Prod. Plant Resour.*, 5 (3), 18-22.

Wang et al., 2012 – *Wang L., Peng S., Danence L. J. T., Gao Y., Wang J.* (2012). Amine-Catalyzed [3+2] Huisgen Cycloaddition Strategy for the Efficient Assembly of Highly Substituted 1,2,3-Triazoles. *Chem. Eur. J.*, 18, 6088-6093.

Yanai et al 2004 – *Yanai T., Tew D.P., Handy N.C.* (2004). A new hybrid exchange? correlation functional using the Coulomb-attenuating method (CAM-B3LYP) Chemical Physics Letters, 393: 51-57.

Zaki et al., 2017 – *Zaki M., Oukhrib A., Akssira M., Berteina-Raboin S.* (2017). Synthesis of novel spiro-isoxazoline and spiro-isoxazolidine derivatives of tomentosin. *RSC Adv.*, 7, 6523-6529.

Zeroual et al., 2014a – *Zeroual A., El Idrissi M., Benharref A., El Hajbi A.* (2014). Theoretical study of regioselectivity and stereoselectivity of condensation of β-himachalene with dichlorocarbene using density functional theory (DFT*). International Journal of Innovation and Applied Studies,* 5 (2), 120-130.

Zeroual et al., 2014b – *Zeroual A., Hammal R., Benharref A., El Hajbi A.* (2014). A theoretical investigation of the regio- and stereoselectivities of the β-himachalene. *Journal of Computational Methods in Molecular Design*, 4 (3), 106-112.

Zeroual et al., 2014c – *Zeroual A., Hammal R., Ryachi K., Barhoumi A., Benharref A., El Hajbi A.* (2014). Understanding the Regioselectivity and Reactivity of β-Himachalene Using Zeroual Function as a new Regioselectivity Descriptor. *International Journal of Innovation and Applied Studies*, 8 (2), 750-755.

Zeroual et al., 2015a – *Zeroual A., Barhoumi A., Bakkas S., El Hajbi A.* (2015). Understanding, which oxygen attacks bromotrimethylsilane in McKenna Reaction using DFT calculation? *Journal of Computational Methods in Molecular Design*, 5 (3), 150-154.

Zeroual et al., 2015b – *Zeroual A., Benharref A., El Hajbi A. (2015).* Theoretical study of stereoselectivity of the [1+2] cycloaddition reaction between (1S,3R,8S)-2,2-dichloro-3,7,7,10-tetramethyltricyclo[6,4,0,01.3]dodec-9-ene and dibromocarbene using density functional theory (DFT) B3LYP/6-31G*(d). *Journal of Molecular Modeling, 21 (3), 1610-2940.*

Zeroual et al., 2015c – *Zeroual A., El Haib A., Benharref A., El Hajbi A.* (2015). A Combined Experimental and Theoretical Study of highly chemioselectivity acetylation of diterpene. *Journal of Computational Methods in Molecular Design*, 5 (3), 58-62.

Zeroual et al., 2015d – *Zeroual A., El Hajbi A.* (2015). Understanding the regioselective and molecular mechanism of the TCE in cycloaddtion reaction (TCE+Cp) and addition reaction (TCE+HCl) using DFT calculation. *Canadian Chemical Transactions,* 3 (4), 430-437.

Zeroual et al., 2015e – *Zeroual A., Hammal R., Benharref A., El Hajbi A.* (2015). The regio- and stereoselective addition of dibromocarbene and dichlorocarbene onto β-himachalene. *Mor. J. Chem.*, 3(4), 698-704.

Zeroual et al., 2015f – *Zeroual A., Hammal R., El Hajbi A.* (2015) A DFT Study of the [1+2] Cycloaddition Reactions of 2-[1, 3]Dioxolan-2-ylidene-malononitrile, TCE and chlorocarbene. *Journal of Computational Methods in Molecular Design.*, 5 (4), 97-101.

Zeroual et al., 2015g – *Zeroual A., Mazoir N., Benharref A., El Hajbi A.* (2015). Understanding of the stereoselective epoxidation on triterpene derivative using transition state theory. *Journal of Computational Methods in Molecular Design.*, 5 (4), 158-161.

Zeroual et al., 2015h – *Zeroual A., Zoubir M., Hammal R., Benharref A., El Hajbi A.* (2015). Understanding the regioselectivity and reactivity of Friedel–Crafts benzoylation using Parr functions". *Mor. J. Chem.* 3(2), 356-360.

Zeroual et al., 2016 – *Zeroual A., Hammal R., Benharref A., Mazoir N., El Hajbi A.* (2016). A theoretical investigation of the reactivity and regioselectivity of triterpene derivatives using difference local index, Parr functions and a difference of Parr functions. *Mor. J. Chem.*, 4 (4), 938-944.

Zeroual et al., 2017a – *Zeroual A., El Idrissi M., El Ajlaoui R., Ourhriss N., Abouricha S., Mazoir N., Benharref A., El Hajbi A.* (2017). MEDT study of the mechanism and regioselectivity of diazocompounds and alkenes in [3+2] cycloaddition reaction". *European Journal of Molecular Biotechnology,* 5(1), 43-49.

Zeroual et al., 2017b – *Zeroual A., El Idrissi M., Zoubir M., Benharref A.* (2017). Theoretical study of the reactivity and regioselectivity of the addition reaction between HCl and alkenes, investigation of the Markovnikov's rule. *European Reviews of Chemical Research*, 4(1), 21-27.

Zeroual et al., 2017c – *Zeroual A., El Idrissi M., Zoubir M., El Ajlaoui R., Abouricha S., El Hajbi A.* (2017). Theoretical Study of the Mechanism and Regioselectivity of Prop-2-Yn-1-Ol with Azide in [3+2] Cycloaddition Reactions. *Open Access Journal of Translational Medicine & Research*, 1(1), 1-5.

Zeroual et al., 2017d – *Zeroual A., Zoubir M., El Idrissi M., El Ajlaoui R., El Haib A., Abouricha S., Mazoir N., El Hajbi A.* (2017). Theoretical Analysis of Reactivity and regioselectivity in [1+2] cyloaddtion reaction of limonene, terpinolene and γ-terpinene with dichlorocarbene, *Global Journal of Science Frontier Research: B, Chemistry*, 17(1).

Zoubir et al., 2016 – *Zoubir M., Zeroual A., Benharref A., El Hajbi A.* (2016). Understanding the Holleman Rule in the Electrophilic Substitution Reaction Using Parr Functions. *Journal of Computational Methods in Molecular Design*, 6 (4), 1-4.

Zoubir et al., 2017a – *Zoubir M., El Idrissi M., El Ajlaoui R., El Haib A., Zeroual A., Benharref A., El Hajbi A.* (2017). Theoretical study of the chemo and the regioselectivity of the Baeyer-Villiger reaction of bicyclo[3.2.0]hept-2-en-6-one by hydrogen peroxide. *European Reviews of Chemical Research*, 4(1), 28-33.

Zoubir et al., 2017b – *Zoubir M., Zeroual A., El Idrissi M., Bkiri F., Benharref A., Mazoir N., El Hajbi A.* (2017). Experimental and theoretical analysis of the reactivity and regioselectivity in esterification reactions of diterpenes (totaradiol, totaratriol, hinikione and totarolone), *Mediterranean Journal of Chemistry*, 6(4), 98-107.

Zoubir et al., 2017c – *Zoubir M., Zeroual A., El Idrissi M., El Haib A., Moumou M., Hammal R., Mazoir N., Benharref A., El Hajbi A.* (2017). Understanding the chemoselectivity and stereoselectivity in Michael addition reactions of β-hydroxyparthenolides and amines such as pyrrolidine, morpholine, piperidine and 1-methylpiperazine: a DFT study. *J. Mater. Environ. Sci.*, 8(3), 990-996.

Published in the Slovak Republic
European Journal of Molecular Biotechnology
Has been issued since 2013.
E-ISSN: 2409-1332
2019, 7(1): 17-24

DOI: 10.13187/ejmb.2019.1.17
www.ejournal8.com

Grouping of Proteins Comprised in the Lungs Proteome by Physico-Chemical and Functional Properties of *Bos Taurus* and *Sus Scrofa*

Pavel A. Krylov [a, *], Nikita I. Stepanenko [a], Natalia A. Borozdina [a]

[a] Volgograd State University, Russian Federation

Abstract

The article is concerned with lungs proteome analysis of live-stock animals (*Bos Taurus* and *Sus scrofa*) with further proteins grouping by their physico-chemical and functional properties. Primary information of proteins comprised in the lungs proteomes of *Bos Taurus* and *Sus scrofa* was obtained from the UniProt database, taking into account the functional properties received from Gene Ontology database. The analysis revealed several thousand annotated proteins used for further grouping: by the chemical nature of their prosthetic groups, their localization in relation to the cell and functional properties. Consequently, we found a predominance of phosphoproteins in the lungs proteome, exceeding by almost 2 and 10 times the number of proteins related to glycoproteins and lipoproteins, respectively. Protein analysis by their localization in relation to the cell reveals a predominance of membrane and intracellular proteins. Practically significant proteins were extracellular proteins. Maximum function diversity of proteins comprised in the lungs proteome was in *Bos Taurus* - 741, *Sus scrofa* – 379. Therefore, lungs proteins of *Bos Taurus* are more promising for the industrial production than *Sus Scrofa's* ones. The obtained data can be used as a basis for the development or optimization of protein isolation methods for the pharmaceutical and biotechnology industries demands in future.

Keywords: proteome, databases, UniProt, Gene Ontology, physico-chemical properties, *Bos Taurus*, *Sus scrofa*.

1. Introduction

Lungs of live-stock animals such as cows and pigs are the product of secondary meat processing in animal husbandry. Accordingly, discussions on rational use concerning thesecondary animal products processing are under way (Faustino et al., 2019). Currently pharmaceutical and biotechnological products of the proteins isolated from the live-stock animals lungs are used. For example, one of the medicines is Calfactant, which contains surfactant proteins B and C (Ga et al., 2015; Bayat et al., 2015; Speer et al., 2013; Chen et al., 2016), and medicines, which contain Aprotinin (Baoukina et al., 2010; Mahdy et al., 2004; Wagener et al., 2008; Jegadeesan et al., 2016). Nevertheless apart from surfactant-associated proteins in the lungs, there are other promising proteins which can be used in the new therapeutic strategies development.

Complete proteome analysis based on functional and physico-chemical properties with the further development of protein isolation and purification methods is required with the purpose of finding promising proteins (Qoronfleh, 2004; Thysen et al., 2015). Particular difficulties may arise in the process of cellular and membrane-bound animal proteins isolation and purification from whole cells extracts. Regardless of the reason for the particular protein isolation and purification,

* Corresponding author
E-mail addresses: p.krylov.volsu@yandex.ru (P.A. Krylov)

the general stages are basically the same. Nevertheless applying of methods certain modifications to specific problems, such as protein insolubility and the loss of its activity, which can be encountered during the isolation and purification processes, is necessary due to the protein properties. Accordingly, the physico-chemical properties analysis of proteins comprised in the live-stock animals lungs proteome, will enable the development of isolation methods.

In connection with the above, the aim of the study was creation a grouping of proteins by functional and physico-chemical properties comprised in the lungs proteome of *Sus scrofa* and *Bos Taurus*.

2. Materials and methods

Grouping of proteins comprised in the lungs proteome of live-stock animals *Sus scrofa* (pig) and *Bos Taurus* (bovine) was executed by the chemical nature of prosthetic groups, physiological nature and their localization in relation to the cell, and by their functions. The search and analysis of the lungs proteomes was executed using the UniProt database (https://www.uniprot.org). The grouping included only annotated proteins.

Grouping of proteins by the prosthetic groups chemical nature was carried out due to their belonging to glycoproteins [KW-0325], lipoproteins [KW-0449] and phosphoproteins [KW-0597]. Grouping by localization of the target proteins in relation to the cell was carried out using the synonymic construct «Subcellular location» with the key words: cytoplasm «(Cytoplasm [SL-0086])» and cytosol («Cytosol»), membrane («Membrane»), extracellular protein («Extracellular»).

Advanced search query was used in the UniProt database with the inclusion of the identification numbers of the Gene Ontology database (https://www.ebi.ac.uk/QuickGO/) for the purpose of grouping by functional properties. Search of identification GO numbers was carried out using synonymic constructs «lung». The next step was determination of the most common Gene Ontology identification numbers in the lungs proteome.

Excel (Microsoft Office, USA) was used in building summary tables based on the results of analysis and grouping. The tables included the following elements: organism name, Uniprot ID, prosthetic groups chemical nature, physiological property (enzyme/receptor), their localization in relation to the cell and functions.

3. Results and discussion

As a result of the UniProt database bioinformatic analysis, 472 annotated proteins of *Bos taurus* and 193 – of *Sus scrofa* comprised in the lungs proteome were obtained. After the analysis of the received proteins, they were assorted by the prosthetic groups chemical nature for *Bos taurus* (Table 1) and *Sus scrofa* (Table 2)

Table 1. Grouping of proteins comprised in the lungs proteome of *Bos Taurus* by the prosthetic groups chemical nature

Glycoproteins (158)
P35246, O46406, Q8SPU5, Q0VCX4, Q2KJH1, P30922, P21758, Q3T0I2, F1MMS9, P79391, P21809, P24627, Q5E9P3, O19116, Q9XT49, Q06599, P21214, P79331, O97827, Q28044, Q10741, Q17QB3, O97831, P42891, O77783, P25930, P39873, F1MJW3, A5D7U4, P51867, Q1JQA4,Q32KP1, A6QLF8,Q3ZBV0, Q704V6, Q0VCF5, Q3T0Q2,Q9GLX9, A7YWH9,Q3SZE3, Q9TQZ3, Q28173, Q2KJ39, A4D7S0, Q3ZBN5, Q2HJ17, Q0II78, Q3ZBH3, Q3LUH2,Q9XSK2, Q2KIV9, Q5E9E3, P85521, P46626, Q5EA66, O77802, P22444, P10730, Q8SPF8, O77750, P35350, Q1RMR1, A2VDP5, Q11126, Q2KIX5, P21450, Q95M17, Q0VCS6, P11052, A6QP79, B9VR26, P32749, A6QLI0, Q5EA62, P98133, P56541, A6QLZ7, A5D7H3, A7MB63, Q29RT9, Q95122, Q9MZ08, P26201, Q5E9X0, Q0VCA0, P14769, Q5E9H1, P58354, P04651, Q0VCP3, Q32PI9, P31096, Q8SPJ1, Q58D34, Q58D84, P50291, P26892, P20959, Q05716, Q28028, P52173, A7MB64, Q5J316, Q9MYY0, P30546, Q5BIM9, Q1JQB3, Q28034, Q8SQG8, Q6UC88, Q3T181, P79345, Q0P5F0, P81265, P13909, Q2KJ15, A7MBJ4, Q3MI05, **P15781**, P21793, O62664, Q8WMP9, Q9TTY5, Q9MYW0, Q1LZE9, P45478, Q1JQA0, P30931, Q06807, P20414, Q6QUN5, Q32L50, **Q6RXL1**, A0JNP2, A0JNN2 P55270, Q2KJH6, Q05588, P48616, P02784, P55918, O77836, O77482, Q04790, Q148L1, A5PK45, P32592 Q862A9, P53712, Q0VCJ8, Q769I5, Q5EA06, Q92180, P80746, Q9XT56, A2VE13, Q148M6, Q8HXQ5
Lipoproteins (34)
P28088, F1MMS9, P79391, Q5E9P3, Q06599, P11023, P79132, Q28044, Q2KJ93, P26201, P60519, Q8SQG8, P84080, Q3ZBW5, O77750, Q2HJ17, Q04790, Q95122, P30931, P24275, A4D7S0, Q05588, P46626, Q9XSK2, Q58DW6, P50154, Q3ZBH3, Q1JPA0, Q5E9X0, Q5E9F0, P29105, **P15783**, Q58DS9, Q5EA55
Phosphoproteins (203)
P28088, Q0VCX4, Q2KJH1, P00516, O77834, P21758, P48644, P67868, F1MMS9, Q05717, Q28156, Q5E9P3, Q3T0E7, Q9XT49, Q06599,Q28021, O18971, P11023, P79132, Q66WT7, O97827, Q17R13, Q28044, Q10741, P21146, P17870, Q56K14, Q3T0L7, P61257, F1MJW3, A5D7U4, Q5E9F5, Q3ZBV0,Q0VC58, Q5E988, Q148E7, P50227, Q3ZC34, A7YWH9, A7YY57, Q3SZE3, Q3ZBW5,Q0P5H5, Q3T003, Q0VCC0, Q2HJ17, Q3SZX4, A4FV37,Q2KI22, Q0VCN0,Q765N9, Q1LZF8,A2VDY3, O02754, Q5E9J5, P02817, A4FV29,A2VDP1, P85521, P04272, P21398, Q3T013, Q17QW1, O77750, P48034, P35350, P24275, O97831, A5D7D1,Q9N0W2, P31976, A4IFD2, A5D7A0, P42891, Q2KIT4,Q29S22, Q2KIX5, P21450, P68103, A5D7U0, Q92176,B9VR26, Q2KJ93, Q08E26, P32749, O46382, Q2KIC2,Q8HYW0, P55052, A6QLZ5, P98133, Q0VCQ1, A5D7H3,P25930, Q2KJ36, Q3B7L5, Q9MZ08, Q3T0A6, P19803,P60519, Q1KZG4, Q3SZH7,Q17QE2, A7E3Q8, Q32PI9, P31096, Q8SPJ1, Q5E9E2,Q1LZ74, Q08E02, Q58D84, P03969, P43249, A7YWP4,P26892, P20959, Q05716, Q3ZC46, P30546, Q28034,A4FV08, A0JND2, Q08DU9, Q0VCL6, Q3B7N9, Q3T181, Q2HJ49, Q3T0C8, P81265,O46404, A7MBJ4,E1BM58, Q8MJG1, A6H772, Q66LN0,Q9XT96, Q8WN55,Q9BGI1, Q0P5J0, Q2HJG5, A2VDK6, Q9MYW0, O97681, P21752, O18883, Q8HYY4, P55859,Q32PF3, Q2KJ28, Q3T0T1,Q3ZBP3, Q3ZBF7, Q27967,Q3MHG1, Q05B92,Q9GMB8, Q3ZBT5, Q06807, P20414,Q2KIC8, Q3T0D7, A5D7K1, Q3SWZ6, P82915, Q2HJ86,A3KMV1, Q2KI99, Q2KJH6, E1BJD1, Q1JQE0, P67808,P48616, Q9BEG9, Q32LP7, Q2KJE0, Q2KJA1, Q3T0Q8,F1MJM0, P46196, Q0VCF9, O77836, Q9GLE4, Q04790,Q0VBZ5, Q8MKF0, Q5EAE5, P32592, Q29S21, Q5GJ77,P53712, Q2KI23, Q769I5, P11017, Q9BDR7, P01966,Q9XT56, P02070, A1A4R1, Q0VBY8, Q148M6, Q27966, Q28824, Q8HXQ5

Note: surfactant-associated proteins are highlighted in bold

Table 2. Grouping of proteins comprised in the lungs proteome of *Sus scrofa* by the prosthetic groups chemical nature

Glycoproteins (78)
Q9N1X4, Q5XW65, Q29411, P23563, P09858, O77633, O46427, Q28997, Q764M9, P20735, Q29055, Q6RHW4, Q5I2M3, P07200, P02543, Q02745, P21692, P53714, Q5U9S1, O02671, Q1W675, Q8SQ34, Q95L12, P52649, O97763, Q9MYU4, P26445, Q6KEQ9, Q75ZH0, Q9TUQ3, Q764N2, Q5PXD3, Q3ZDR4, Q95252, Q8HYN8, 8WN93,A9Y006, A8W649, Q2VL90, Q8MIB3, P30555, Q10982, Q9MYZ9, P35463, Q58D68, Q29010, B1PHQ8, B6CVD7,Q9TV36, Q29121, F1S584, Q29243, O62680, P14082, P50127, Q29042, A7UHZ5, Q95J68, A2BD09, Q8WNW3,Q9MYM5, P18430, Q29056, P01219, B3SP85, P79335, Q9XSD4, Q9N2D1, Q95242, Q6TYI6, Q5MNU5, **P49874**, Q28983, Q9GJR5, P01232, P79385, Q01580, Q1RPR6
Lipoproteins (16)
Q007T2, P23563, Q4LE85, Q52NJ, Q28997, Q007T5, P00592, P26234, Q6RVA9, Q06AU3, P3546, Q58D68, Q95252, O62680, P30555, Q8HYN8
Phosphoproteins (93)
Q29529, Q007T2, O62807, P19619, Q29073, Q19S50, P23563, P63053, O46374, Q4LE85, A5D9M6, A5GFW1, O77633, Q28997, Q764M9, I3LM39, Q8WNV7, Q2VIU1, Q9TUB2, Q9TU45, B8XX90, P26234, P02543,P21692,Q9XT90,P53714,Q2YGT9,Q95342,P80220,C5HGF3,F1SR90,A5GFW7,Q2HY40, P21753,Q95274,Q3S853,A5GFN6,Q06AU3,A5GFW5,Q6RVA9,P35750,Q764N2,Q5PXD3,Q8WN 93,O19004,Q2VL90,P30555,Q9MYZ9,P35463,Q58D68,Q29010,P13222,P67872,P52649, B1PHQ8,P04574,B6CVD7,Q9TV36,F1S584,P52650,Q29243,B0KYV5,Q5PXT2,P12675,Q7YR76, Q8WNW3,P60662,Q8MJ49,Q29024,Q1W675,P18430,A0FIN4,P80031,P61291,Q9TSX9,Q6R2V 0,Q95242,P67937,Q4VYA0,I3L5V6,Q6QAP7,Q5MNU5,Q767L7,P00339,O02671,Q9GJR5,Q8MJ 39,Q9XSZ6,P01965,P02067,P62802, Q71LE2,Q29122

Note: surfactant-associated proteins are highlighted in bold

As a result of the proteins grouping by their localization in relation to the cell, there was a significant predominance of proteins associated with membranes both in *Bos taurus* (Table 4), and *Sus scrofa* (Table 3).

Table 3. Grouping of proteins comprised in the lungs proteome of *Sus scrofa* by the localization in relation to the cell

Cytoplasm (60)
Q29411, Q007T2,O62807, P19619,Q29073, Q19S50,P63053, A5D9M6,A5GFW1, Q6QAQ1,Q007T5, I3LM39, P16469, Q2VIU1,Q9TUB2, B8XX90,P26234, P02543,Q9XT90, Q9N1F5,Q29122, P35750,P00339, Q9TSX9, P26889, Q06AU3,Q2YGT9, P83884,Q95342, P80310,P80220, F1SR90,Q2IA00, P35323,Q2HY40, P21753, Q95274, P46405,Q3S853, A5GFN6,A5GFW5, A3QRX8,P04574, Q29243,D2SW95, B0KYV5,Q5PXT2, Q8WNW3,Q8MJ49, Q29024,Q8MJD6, A0FIN4,P80031, P61291,Q6R2V0, P67937,I3L5V6, Q28999, Q767L7, P12309
Membrane (82)
Q007T2, P19619, P23563, Q4LE85,Q52NJ1, O77633,Q28997, Q007T5,Q764M9, I3LM39,P20735, P16469,Q9TU45, Q5I2M3,B8XX90, P26234,Q02745, Q9XT90,P53714, Q9XSZ6,Q29122, O02671,Q1W675, Q8SQ34,P35750, Q6RVA9,P80310, P26445,C5HGF3, F1SR90,Q3S853, Q6KEQ9,Q06AU3, Q75ZH0,Q764N2, Q5PXD3,Q3ZDR4, Q95252,Q35916, Q8HYN8,Q8WN93, A9Y006,A8W649, Q2VL90,Q30C86, Q8MIB3,P30555, Q10982,Q9MYZ9, P35463, Q9MYU4, Q58D68, Q29010,P52649, B1PHQ8,P04574, B6CVD7,Q29121, F1S584,P52650, Q29243,O46420, Q29036,D2SW95, O62680,P50127, Q29042,B0KYV5, Q8WNW3, Q9XSD4,Q767L9, Q95242,Q6TYI6, Q5MNU5, P47787,O97562, Q28983,Q9GJR5, P79385,Q01580, Q1RPR6,P82126

Extracellular space (12)
Q9N1X4,Q29411,P19619,P09858,P07200,P21692,Q29243,Q9TV36,Q01580, P45846, **P49874**, Q29042

Note: surfactant-associated proteins are highlighted in bold

Table 4. Grouping of proteins comprised in the lungs proteome of *Bos Taurus* by the localization in relation to the cell

Cytoplasm (125)
Q0VCX4, P00516, O77834, P30922, P48644,P16068, Q08E39, P79105,Q28021, O18971, P11023, Q66WT7, P62739, P21146, P17870, P48034, P31976, P18203, Q92176, Q2KJ93, Q3B7L5, P79135, Q8SPJ1, Q08E02, P43249, Q3ZC46, Q4U5R4, P50227 , Q0P5H5, Q0VCC0, Q3SZX4, A4FV37, Q2KI22, Q27971, O02751, A2VE78, Q3SX44, Q58CQ2, O18737, P84080, Q17QW1, P63258, A5D7D1, A2VDX7, Q2KIT4, Q2KIX5, P68103, Q95M17, A5D7U0, Q0VCQ0, Q08E26, O46382, P55052, Q2KJ36, Q3SZT6, P19803, P19687, Q1KZG4, O18879, Q3SZH7, Q17QE2, A7E3Q8, F1N152, Q8MJD5, P68265, A4FV08, Q2HJ49, Q0VCN1, Q5E9B6, Q3T0C8, P05980, E1BM58, Q3T0E7, A6H772, Q66LN0, P52897, Q9BGI1, Q0VCW6, A2VE79, Q2HJG5, A2VDK6, P21752, O18883, Q8HYY4, P55859, Q3T0T1, Q0VCJ7, O02739, Q5BIR5, Q3ZBF7, Q9GMB8, Q17QV3, Q06807, Q3ZCC8, Q3MHL6, Q2KIC8, Q28050, P28782, A5D7K1, Q3SWZ6, Q2HJ86, P55270, Q2KI99, Q0VCI2, P67808, P48616, Q5E969, Q3MHQ4, Q32LP7, Q2KJA1, P46196, Q9GLE4, Q8MKF0, Q5EAE5, A5PKK7, Q148C9 ,Q58DS6, Q56JY0, Q28035, P11017, Q9N0V4, Q3T0K9, Q148M6, Q27966, Q28824
Membrane (195)
P28088, Q0VCX4,P21758, F1MMS9, P79391, Q5E9P3, Q08E39, P79105, Q9XT49, Q06599, Q28021, P11023, P79132, Q66WT7, Q7SIB2, O97827, Q17R13, Q28044, Q10741, P21146, P17870, P04272, O97831, P31976, P42891, P18203, F1MJW3, A5D7U4, Q3SYU3, Q5EA70, P51867, Q1JQA4, Q32KP1, A6QLF8, Q3ZBV0, Q704V6, A0JNK6, Q0VC58, Q0VCF5, Q3T0Q2, Q8HZT6, A7YWH9, Q3SZE3, Q9TQZ3, Q28173, Q3ZBW5, Q0P5H5, Q58DW6, Q3SZI5, Q2HJ17, Q0II78, A4FV37, Q2KI22, Q3ZBH3, Q27971, Q3LUH2, Q0VCN0, Q765N9, Q2HJ22, Q29442, Q9XSK2, Q1LZF8, A2VDY3, Q5E9J5, O18737, P84080, P85521, P46626, P10730, P21398, Q3T013, Q17QW1, O77750, P35350, P24275, Q148F2, Q1JPA0, Q9N0W2, A2VDP5, Q11126, A5D7A0, Q2KIT4, Q2KIX5, P21450, P68103, Q0VCS6, A6QP79, Q92176, B9VR26, Q2KJ93, Q0VCQ0, O46382, A6QPI4, O77783, P55052, A4IFP3, A5D7H3, P25930, Q2HJ66, A7MB63, Q29RT9, Q3SZT6, Q95122, Q9MZ08, P26201, Q3ZCD0, Q5E9X0, Q01888, P14769, Q5E9F0, P58354,Q0P5F3, Q32PI9, P79135, Q5E972, Q1RMT9, Q3SYT0, Q8SPJ1, P43249, F1N152, Q5I3B2, A7MB64, Q5J316, Q9MYY0, P30546, Q5BIM9, Q1JQB3, Q8SQG8, P29105, Q24JY7, Q6UC88, Q3T181, Q2HJ49, Q0P5F0, P81265, A7MBJ4, E1BM58, A6H7B8, Q0VCC1, Q66LN0, Q9XT96, O62664, Q95L14, Q8WMP9, Q58DS9, Q9TTY5, Q2HJG5, Q9MYW0, O97681, Q27979, Q3MHG1, P30931, Q0IIE5, Q3ZBT5, Q06807, Q6QUN5, Q2KIC8, P28782, Q1LZB3, P55270, Q2KI99, Q0VCI2, Q05588, A1A4L0, A1A4J8, Q2KJA1, P81103, P46196, O77836, Q9GLE4, Q6IED8, Q04790, Q8MKF0, Q5EAE5, Q6QRN8, Q148L1, P32592, Q862A9, Q5GJ77, P53712, Q769I5, A4IF94, P50154, Q5EA06, O18756, Q92180, Q9BDR7, P80746, Q5EA55, Q9XT56, A2VE13, Q95J56, Q148M6, Q27966, Q8HXQ5
Extracellular space (24)
P35246, O46406, Q2KJH1, P30922, P21809, P21214. P79331, Q7SIB2, P04272, P21793, P98133, A4D7S0, P02817, Q29442, **P15781**, **Q6RXL1**, Q9GLX9, **P15783**, O18739, Q5EA62, P55918, Q3ZBN5, Q32L50, **P00974**

Note: surfactant-associated proteins and aprotinin are highlighted in bold

Thereby, correlation between cytoplasmic proteins, associated with the membrane and located in the extracellular space, is almost the same both in *Bos taurus* and *Sus scrofa*. Proteins with practical significance are represented by glycoproteins/lipoproteins and they are located in the extracellular space, upon a detailed proteins exploration, for example, P35246 – Pulmonary surfactant-associated protein D and P00974 – Pancreatic trypsin inhibitor (Aprotinin).

As a result of the search for identification numbers, associated with the proteins functional properties in Gene Ontology, 31 identifiers were found. Only 8 of them are associated with proteins

comprised in the lungs proteome of *Bos Taurus* and *Sus scrofa*: GO:0061033, GO:0030324, GO:0060437, GO:0060428, GO:0060487, GO:0048286, GO:0060449, GO:0060501.

Consequently, the most common proteins functions, presented in Figure 1, were revealed.

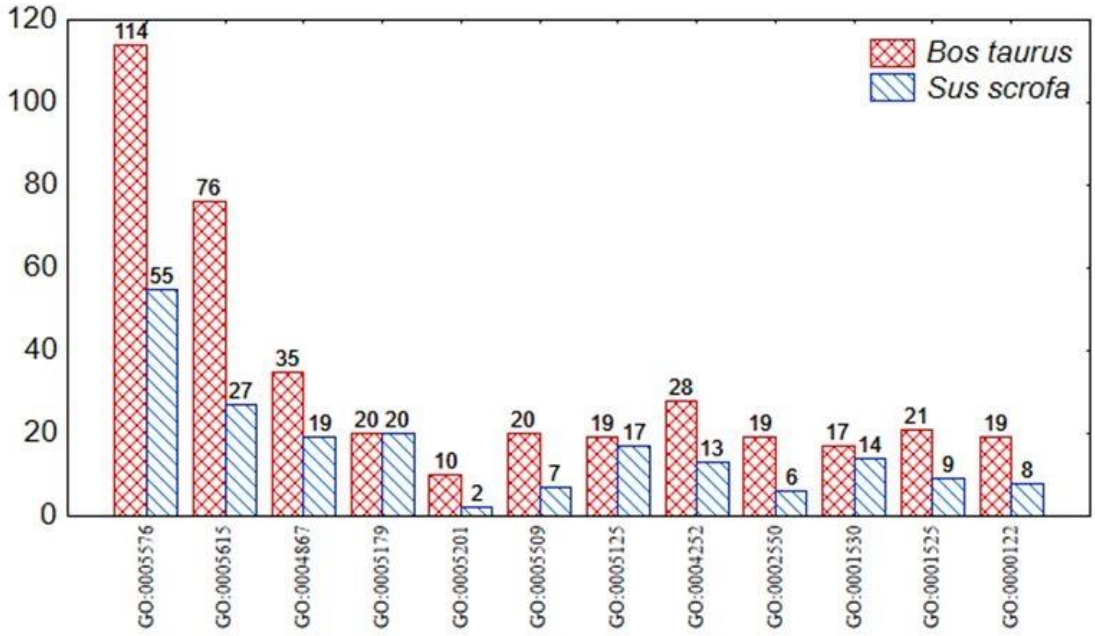

Fig. 1. The most frequently occurring functional properties of proteins, comprised in the lungs proteome of *Bos Taurus* and *Sus scrofa*, according to Gene Ontology

Maximum function diversity of proteins comprised in the lungs proteome is in *Bos Taurus* – 741, *Sus scrofa* – 379. Predominately, there are proteins excreted into the extracellular space, and proteins involved in the endopeptidase activity regulation process. Proteins related to group GO: 0004867 get involved in cell adhesion, extracellular matrix formation. Among the proteins of GO: 0005615 group, there were founded proteins-regulators of cell differentiation and proliferation, transport proteins and lipoproteins and proteins associated with lipids. Proteins involved in cell adhesion were founded in both the GO: 0005576 and GO: 0005615 groups. Proteins of GO: 0004867 group are inhibitors of metalloproteinases, serine and trypsin proteases, chymotrypsin, thrombin and express endopeptidase activity. Collagen and proteoglycan chains are also frequently occurring proteins.

Accordingly, the isolation of proteins from the lungs of *Bos Taurus* for the purpose of exploration will be more effective, than from the lungs of *Sus Scrofa*. The major part of the proteins is hydrophobic and interacts with lipids or is lipoproteins, what should be taken into account in isolation and purification.

As for the molecular weight, the correlation between proteins functions of GO: 0005576 and GO: 0005615 groups were not found. Proteins of GO:0004867 can be divided by mass into three groups:

1. Structural proteins involved in the synthesis and fixation of hyaluronic acid in the extracellular space: have the largest molecular weight – 100-104 kDa.

2. Hydrophobic proteins, which are responsible for the proteinase inhibitors transport, – 44–46 kDa.

3. Proteases inhibitors (trypsin, acrosin, plasmin, serine protease) – 6-14 kDa.

Consequently, proteins separation by molecular weight using electrophoresis can be the basis for their division by functional properties.

Maximum number of proteins of *Bos Taurus* and *Sus scrofa* depending on their localization in relation to the cell is membrane ones. They are divided into peripheral and integral membrane proteins, which are associated to varying degrees with the phospholipid bilayer. Peripheral membrane proteins can be dissociated using relatively mild techniques that break the electrostatic

or hydrogen bonds between the peripheral proteins and the membrane, without total membrane disruption. For this purpose buffers containing high salts are used as they decrease electrostatic interactions between proteins and charged lipids. Chaotropic ions disrupt hydrophobic bonds present in the membrane surface and promote the transfer of hydrophobic groups from non-polar environment to the aqueous phase (Pandey et al., 2016).

In order to solubilise integral membrane proteins, it is necessary to disrupt the lipid bilayer, which may be achieved with organic solvents.

In the proteins distribution, depending on prosthetic groups, the majority was represented by phosphoproteins. Ion-exchange chromatography or chromatofocusing, affinity chromatography with immobilized metals are used for proteins isolation and purification (Adamczyk et al., 2001).

In previous studies, surfactant-associated proteins and Aprotinin, which have practical importance, were discovered in the result of proteome analysis using virtual screening. Knowledge about physico-chemical, physiological properties and information about pulmonary proteins localization in relation to the cell can help to predict the possibility of practically significant proteins isolation and purification.

4. Conclusion

Knowledge of physico-chemical properties are necessary for isolation potentially significant proteins from the lungs. Frequently occurring lungs proteins are phosphoproteins and lipoproteins, located on cell membranes, or secreted into the extracellular space. This feature should be taken into account in the proteins isolation, and isolate the proteome in two stages – with the extraction of hydrophobic, and hydrophilic proteins from the lungs.

The proteome analysis performed in this work will allow to create a strategy for the isolation and purification of proteins mainly from the lungs of *Bos Taurus*, as this organism has maximum functional diversity of proteins and the largest number of annotated proteins in physico-chemical properties.

5. Acknowledgments

This work was supported by the Russian Foundation for Basic Research (RFBR) Project no. 18-44-343003 “Complex potentially bioactive molecules isolation, based on the study of cattle lungs proteome”

References

Adamczyk et al., 2001 – *Adamczyk M., Gebler J.C., Wu J.* (2001). Selective analysis of phosphopeptides within a protein mixture by chemical modification, reversible biotinylation and mass spectrometry. *Rapid Communications in Mass Spectrometry*, 15(16), 1481-1488

Baoukina et al., 2010 – *Baoukina S., Tieleman D.P.* (2010). Direct simulation of protein-mediated vesicle fusion: lung surfactant protein. *B. Biophysical Journal.*, 99(7), 2134-2142. DOI: 10.1016/j.bpj.2010.07.049

Bayat et al., 2015 – *Bayat S., Porra L., Broche L. et al.* (2015). Effect of surfactant on regional lung function in an experimental model of respiratory distress syndrome in rabbit. *Journal of Applied Physiology,* 119(3), 290-298. DOI: 10.1152/japplphysiol.00047.2015

Chen et al., 2016 – *Chen K.-L., Lv Z.-Y., Yang H.-W., et al.* (2016). Effects of Tocilizumab on experimental severe acute pancreatitis and associated acute lung Injury. *Critical Care Medicine*, 44(8), e664–e677. DOI: 10.1097/CCM.0000000000001639

Faustino et al., 2019 – *Faustino M., Veiga M., Sousa P. et. al.* (2019). Agro-food byproducts as a new source of natural food additives. *Molecules*, 24(6): 1056. DOI: 10.3390/molecules24061056

Ga et al., 2015 – *Ga W.J., Minkyung O., Jong B.S.* (2015). Efficacy of Surfactant-TA, Calfactant and Poractant Alfa for Preterm infants with respiratory distress syndrome: A Retrospective Study. *Yonsei Med J.,* 56(2): 433-439. DOI: 10.3349/ymj.2015.56.2.433

Jegadeesan et al., 2016 – *Jegadeesan V., Ponnaiyan D.* (2016). Impact of Aprotinin – A Proteolyticenzyme on postsurgical symptoms in patients undergoing third molar surgeries. *J. Clin. Diagn. Res.*, 10(1), ZC18–ZC22. DOI: 10.7860/JCDR/2016/15491.7056

Mahdy et al., 2004 – *Mahdy A.M., Webster N.R.* (2004). Perioperative systemic haemostatic agents. *Br J Anaesth.,* 93(6): 842-58. DOI: doi.org/10.1093/bja/aeh227

Pandey et al., 2016 – *Pandey A., Shin K., Patterson R.E. et al.* (2016). Current strategies for protein production and purification enabling membrane protein structural biology. *Biochem Cell Biol.*, 94(6): 507-527. DOI: 10.1139/bcb-2015-0143

Qoronfleh, 2004 – *Qoronfleh M.W.* (2004). Proteomics: the next frontier – a biotech perspective. *J. Biomed Biotechnol.*, (3): 121-123. DOI: 10.1155/S1110724304404094

Speer et al., 2013 – *Speer C.P., Sweet D.G., Halliday H.L.* (2013). Surfactant therapy: past, present and future. *Early Human Development,* 89, S22–S24. DOI: 10.1016/S0378-3782(13) 70008-2

Thysen et al., 2015 – *Thysen S., Luyten F.P., Lories R.J.U.* (2015). Targets, models and challenges in osteoarthritis research. *Disease Models & Mechanisms,* 8: 17-30. DOI: 10.1242/dmm.016881

Wagener et al., 2008 – *Wagener G., Gubitosa G., Wang S.* (2008). Increased incidence of acute kidney injury with aprotinin use during cardiac surgery detected with urinary NGAL. *Am. J. Nephrol.*, 28(4), 576-582. DOI: 10.1159/000115973

Published in the Slovak Republic
European Journal of Molecular Biotechnology
Has been issued since 2013.
E-ISSN: 2409-1332
2019, 7(1): 25-39

DOI: 10.13187/ejmb.2019.1.25
www.ejournal8.com

Polynuclear Heterocyclic Monomethine and Trimethine Cyanine Dyes: Synthesis and Various Absorption Spectra Studies

H.A. Shindy [a, *], M.A. El-Maghraby [a], M.M. Goma [a], N.A. Harb [a]

[a] Department of Chemistry, Faculty of Science, Aswan University, Aswan 81528, Egypt

Abstract

New polynuclear heterocyclic compound namely 4-methyl-2-phenyl-benzo[(2,3-b)benzoxazine; (2', 3'-b')furo(3,2-d)pyrazole]-5,12-dione was designed, prepared and employed as starting material in the synthesis of new methine cyanine dyes, covering monomethine cyanine dyes (simple cyanine dyes) and trimethine cyanine dyes (carbocyanine dyes). The electronic visible absorption spectra of all the synthesized cyanine dyes were investigated in 95% ethanol solution to evaluate their spectral sensitization properties. The electronic visible absorption spectra for some selected dyes were examined in pure solvents having different polarities [Water (78.54), Dimethylformamide (36.70), Ethanol (24.3), Chloroform (4.806), Carbontetrachloride (2.238) and Dioxane (2.209)] and/or in aqueous universal buffer solutions owing varied pH values (1.99, 2.99, 4.30, 6.87, 7.96, 8.91, 10.55 and 12.04 units) to evaluate their solvatochromic and/or halochromic properties, respectively. Structural determination was carried out via elemental analysis, visible, mass, IR and ^{1}HNMR spectroscopic data.

Keywords: cyanine dyes, methine cyanine dyes, synthesis, absorption spectra, solvent effects, acid/base properties.

1. Introduction

In the recent years, a considerable attention have been given to the chemistry of cyanine dyes, dealing with their synthesis, characterizations and applications (Shindy, 2017; Shindy, 2018; Shindy et al., 2019; Arjona et al., 2016; Ashitate et al, 2016; Hyun et al., 2015; Soriano et al., 2015; Sato et al., 2019; Schwechheimer et al., 2018; Rodríguez-Pérez et al., 2017). Essentially, this can be related to the excellent photophysical and photochemical properties of these dyes which makes them easily applicable in a diverse and a broad area of science, technology, engineering, pharmacology and medicine. Cyanine dyes possess two nitrogen containing heterocyclic groups that are connected by a conjugated methine bridge as shown in Figure 1. The delocalization of electrons across this chain causes them to be highly fluorescent and exhibit long wavelength absorption that span from the visible to the near infrared regions (Wyler, 1969; Wyler, 1969a; Musso, 1979; Reichardt, 1995). In past, with the beginning of the 1800s, cyanine dyes were used in photographic emulsions and chemotherapy (Hamer, 1964), and the great commercial value of the cyanine dyes at this time was associated only with their power of conferring extra sensitiveness on silver halide photographic plates. Ordinarily, such plates are sensitive to the violet and blue regions of the spectrum, but adding suitable cyanine dyes to the liquid emulsion or by bathing the dried emulsion film in the dye solution, the plate may be rendered remarkably sensitive to green, yellow, orange, red, and even to the invisible infra-red portions of the spectrum (Dach, Daehne 1997). But

* Corresponding author
E-mail addresses: hashindy2@hotmail.com (H.A. Shindy)

more recently cyanine dyes have been used as functional dyes in high technique fields such as in laser printing (Dähne et al., 1998), pH sensors (Xu et al., 2007), fluorescence *in vivo* imaging (Choi et al., 2011; Choi et al., 2013; Licha et al., 2000; Achilefu, et al., 2000), data storage (Nakazumi, 2008), and as labels for nucleic acid detection (Warner et al., 1996; Haugland et al., 1969; Deligeorgiev et al., 1998).

R=CH_3, CH_3CH_2 ;X=I, Br, ClO_4; n = 0, 1, 2, 3---- etc.

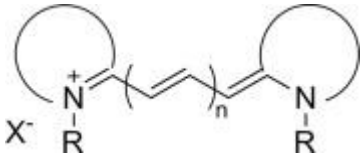

Fig. 1. General structure of cyanine dyes

In this research paper we prepared new polynuclear heterocyclic monomethine and trimethine cyanine dyes as new synthesis contribution and spectrosocopic investigation in the field, and to may be used and/or applied in any of the wide range applications of cyanine dyes, and particularly (according to this study) as photographic sensitizers in photographic material industry (due to their spectral sensitization properties), as probes for determining solvent polarity in solution chemistry (due to their solvatochromic properties) and/or as indicators in operations of acid/base titration in analytical chemistry (due to their halochromic properties).

2. Results and discussion

2.1.Synthesis:

An equimolar ratios of 3,4-dichloro-benzo[b]-phenoxazine-2,5-dione (1) and 3-methyl-1-phenyl-5-pyrazolone (2) were reacted in pyridine and achieved 4-methyl-2-phenyl-benzo[(2,3-b)benzoxazine; (2', 3'-b')furo(3,2-d)pyrazole]-5,12-dione (3) as new polyheterocyclic starting material compound, Scheme (1).

Quaternization of (3) using an excess of iodoethane led to the formation of 3-ethyl-4-methyl-5,12-dione-2-phenyl-benzo[(2,3-b)benzoxazine;(2',3'-b')furo(3,2-d)pyrazolium]iodide quaternary salt compound (4), Scheme (1).

Reaction of the quaternary salt compound (4) with an iodoethane quaternary salts of either pyridine, quinoline or isoquinoline in equimolar ratios and in ethanol containing few drops of piperidine gave3-ethyl-5,12-dione-2-phenyl-benzo[(2,3-b)benzoxazine;(2',3'-b')furo(3,2-d)pyrazole]-4[4(1)]-monomethine cyanine dyes (5a-c), Scheme (1).

Additionally, the quaternized compound (4) was reacted with a unimolar ratios of triethylorthoformate in presence of acetic anhydride and led to the formation of the intermediate compound 3-ethyl-4(1,1'-diethoxyethyl)-5,12-dione-2-phenyl -benzo[(2,3-b)benzoxazine;(2',3'-b')furo(3,2-d)pyrazolium] iodide quaternary salt (6), Scheme (1).

The intermediate compound (6) was further reacted with equimolar ratios of N-ethyl (2-picolinium, quinaldinium, 4-picolinium) iodide quaternary salts in ethanol containing piperidine as a basic catalyst to give 3-ethyl-5,12-dione-2-phenyl-benzo[(2,3-b)benzoxazine;(2',3'-b')furo(3,2-d)pyrazole]-4[2(4)]-trimethine cyanine dyes (7a-c), Scheme (1).

The structure of the prepared compounds were characterized and identified by elemental analysis, Table 1, Visible spectra, Table 1, mass spectrometer, IR (Wade, 1999) and 1H-NMR (Wade, 1999a) spectroscopic data, Table 3.

2.2. Absorption spectra studies in 95 % ethanol solution:

This study was carried out to evaluate the spectral sensitization properties of the synthesized cyanine dyes to may used and/or applied as photographic sensitizers in photosensitive material industry.

The electronic visible absorption spectra of the monomethine cyanine dyes (5a-c) in 95 % ethanol solution discloses bands in the visible region 410-460 nm. The positions of these bands and their molar extinction coefficient (molar absorptivity) are largely influenced by the nature of the heterocyclic quaternary residue (A) and their linkage positions. So, substituting A=1-ethyl pyridinium-4-yl salt in the monomethine cyanine dye 5a by A=1-ethyl quinolinium-4-yl salt to get the monomethine cyanine dye 5b causes strong bathochromic shift by 20 nm, accompanied by increasing intensity of the absorption bands Scheme (1), Table 1. This can be attributed to

increasing π-delocalization conjugation in the latter dye due to the presence of quinoline ring system in correspondance to the pyridine ring system in the former dye.

Changing the linkage positions from 1-ethyl quinolinium-4-yl salt to 2-ethyl isoquinolinium-1-yl salt passing from the monomethine cyanine dye 5b to the monomethine cyanine dye 5c resulted in a remarkable blue shift by 10 nm, Scheme (1), Table 1. This can be explained in the light of decreasing the length of the π-delocalization conjugation in the latter 2-ethyl isoquinolinium-1-yl salt dye 5c compared to the former 1-ethyl quinolinium-4-yl salt dye 5b.

Additionally, the electronic visible absorption spectra of the trimethine cyanine dyes (7a-c) in 95 % ethanol solution discloses bands in the visible region 410-650 nm. The positions of these bands and their molar extinction coefficient are largely influenced by the nature of the heterocyclic quaternary residue (A) and their linkage positions. So, substituting A=1-ethyl pyridinium-2-yl salt in the trimethine cyanine dye 7a by A=1-ethyl quinolinium-2-yl salt to get the trimethine cyanine dye 7b causes strong bathochromic shift by 80 nm, Scheme (1), Table 1. This can be attributed to increasing π-delocalization conjugation in the latter dye due to the presence of quinoline ring system in correspondance to the pyridine ring system in the former dye.

Changing the linkage positions from 2-yl salt to 4-yl salt passing from the trimethine cyanine dye 7a to the trimethine cyanine dye 7c resulted in a remarkable red shifts by 10 nm accompanied by increasing the intensity of the absorption bands, Scheme (1), Table 1. This can be explained in the light of increasing the length of the π-delocalization conjugation in the latter 4-yl salt dye 7c due to the presence of the γ-picolinium structure system compared to the former 2-yl salt dye 7a which contain the α-picolinium structure system.

Comparison the electronic visible absorption spectra of the monomethine cyanine dye (5a-c) with those of the trimethine cyanine dyes (7a-c) reveals that the later trimethine cyanine dyes (7a-c) have strong bathochromic shifted bands accompanied by increasing number of the absorption bands compaired with the former monomethine cyanine dyes (5a-c). This can be related to increasing conjugation due to increasing the number of methine groups between the basic center (nitrogen atom) and the acidic center (quaternary salt) in latter dyes by two methine units, Scheme (1), Table 1.

2.3-Absorption spectra studies in pure solvents having different polarities:

This study was carried out to select the best solvents to use of these cyanine dyes as photosensitizers when there are applied in photographic material industry. The other important purpose of this study is to evaluate the solvatochromic properties of these cyanine dyes to may be used and/or applied as probes for determining solvent polarity, in physical, physical organic, inorganic and/or in solution chemistry.

So, the electronic visible absorption spectra of the monomethine cyanine dye (5b) and trimethine cyanine dye (7b) in pure solvents of different polarities (different dielectric constant) namely water (78.54), dimethylformamide (DMF) (36.70), ethanol (24.3), chloroform (4.806), carbontetrachloride (2.238) and dioxane (2.209) (Shindy, et al., 2014; Shindy, et al., 2014a) are recorded. The λmax (wavelength) and εmax (molar extinction coefficient) values of the absorption bands due different electronic transitions within the solute molecule in these solvents are represented in Table 3.

From Table 3, it is clear that the electronic visible absorption spectra of the cyanine dyes (5b) and (7b) in the ethanolic medium are characterized by the presence of two essential absorption bands (for the dye 5b) and three essential absorption bands (for the dye 7b). These bands can be assigned to intermolecular charge transfer transition (Shindy, et al., 2014; Shindy, et al., 2014a). These charge transfer is due to transfer of lone pair of electrons from the N-ethyl pyrazole nitrogen atoms (the basic and / or the electron pushing center of the dyes) to the positively charged quaternary nitrogen atoms of the quinolinium salts residue, (the acidic and / or the electron pulling center of the dyes) and vice versa, Scheme (2).

The data given in Table (3) show that the charge transfer band exhibits a hypsochromic shift in ethanol relative to DMF, dioxane, chloroform and carbontetrachloride. This effect may be related to the following factors:

a- The bathochromic shifts in DMF relative to ethanol is a result of the increase in solvent polarity due to the increasing of dielectric constant of DMF relative to ethanol.

b- The hypsochromic shift occurs in ethanol relative to dioxane, chloroform and carbontetrachloride is a result of the solute solvent interaction through intermolecular hydrogen

bond formation between ethanol and the lone pair of electrons of the N-ethyl pyrazole nitrogen atoms, Scheme (3) (A). This decreases slightly the electron density on the N-ethyl pyrazole nitrogen atoms and consequently decreases to some extent the moving and mobility of the attached π-electrons over the conjugated pathway to the positively charged quaternary nitrogen atom of the quinolinium salt residue, and consequently a hypsochromic shift occurs.

Also, from the data given in Table 3 it is observed that occurrence of unexpected hypsochromic shifts in water relative to ethanol and the other solvents. This can be mainly ascribed to the possible interaction of water molecules with the lone pair of electrons of the N-ethyl pyrazole nitrogen atoms, Scheme (3) (B). This makes difficult the transfer of electronic charge from the N-ethyl pyrazole nitrogen atoms to the quaternary nitrogen atoms of the heterocyclic quinolinium salt residue, and accordingly there is observed a hypsochromic shift in water relative to ethanol and the other solvents.

2.4-Absorption spectra studies in aqueous universal buffer solutions having varied pH values:

The solutions of the monomethine (5b) and trimethine (7b) cyanine dyes behaves as halochromic compounds where, their ethanolic solutions gives changeable colours in acid/base media being yellow or colourles on acidification and getting back (restore) their original permanent intense colour on basification. This encouraged us to study their spectral behaviour in different buffer solutions to select a suitable pH for use of these cyanine dyes as photosensitizers. The other purpose of this study is to evaluate the halochromic properties of these cyanine dyes in order to identify the possibility of their uses and/or applications as indicators in operations of acid/base titrations in analytical chemistry. The acid dissociation or protonation constants of these dyes have been determined. The effect of the compounds as photosensitizers increase when there are present in the ionic form, which has higher planarity (Shindy, et al., 2014; Shindy, et al., 2014a) and therefore more conjugation.

The electronic visible absorption spectra of the dyes (5b) and (7b) in aqueous universal buffer solutions of varying pH values (1.99, 2.99, 4.30, 6.87, 7.96, 8.91, 10.55 and 12.04 units). showed bathochromic shifts with intensification of their absorption bands at high pH (alkaline media) and hypsochromic shifts with reduction in the intensity of the bands at low pH (acidic media), Table 4.

Therefore the mentioned dyes which have free lone pair of electrons on the N-ethyl pyrazole nitrogen atom undergo protonation in acidic media. This generates positive charge on the N-ethyl pyrazole nitrogen atom, and consequently the electronic charge transfer pathways from the N-ethyl pyrazole nitrogen atom to the heterocyclic quaternary nitrogen atom of the quinolinium salt residue will be greatly affected and difficult resulting in a hypsochromic shift, protonated structures (colourles), Scheme (4) (A).

On increasing the pH of the media, the absorption bands are intensified and bathochromically shifted as a result of deprotonation of the N-ethyl pyrazole nitrogen atom, and accordingly the electronic charge transfer pathways to the quaternary heterocyclic nitrogen atom of the quinolinium salt residue will be easier, facilitated and more favoured resulting in a bathochromic shift, deprotonated structures (coloured), Schemes (4) (B).

Several methods have been developed for the spectrophotometric determination of the dissociation or protonation constants of weak acids. The variation of absorbance with pH can be utilised. On plotting the absorbance at fixed λmax vs pH, S-shaped curves are obtained. On all of the S-shaped curves obtained, the horizontal portion to the left corresponds to the acidic form of the indicator, while the upper portion to the right corresponds to the basic form, since the pka is defined as the pH value for which one half of the indicator is in the basic form and the other half in the acidic form. This point is determined by intersection of the curve with a horizontal line midway between the left and right segments (Shindy et al., 2014; Shindy et al., 2014a). The acid dissociation or protonation constants values of the dyes (5b) and (7b) are listed in Table 5.

3. Conclusion

From the previous discussed results we could conclude that:

1. The electronic visible absorption spectra of the monomethine (5a-c) and trimethine (7a-c) cyanine dyes in 95 % ethanol solution underwent displacements to give bathochromic and/or hypsochromic shifted bands depending upon the following factors:

(A) The nature of the heterocyclic quaternary salt residue in the order of:

i) Quinolinium dyes > pyridinium dyes (in the monomethine cyanine dyes).
ii) Quinaldinium dyes > α-picolinium dyes (in the trimethine cyanine dyes).
(B) Linkage position of the heterocyclic quaternary salt residue in the order of:
i) quinolinium dyes > isoquinolinium dyes (in the monomethine cyanine dyes).
ii) γ-picolinium dyes > α-picolinium dyes (in the trimethine cyanine dyes).
(C) The number of the methine units and/or groups between the two heterocyclic ring system of the cyanine dyes molecules in the order of: trimethine cyanine dyes > monomethine cyanine dyes.

2. The intensity of the colours of the monomethine cyanine dyes, and trimethine cyanine dyes are illustrated according to the following suggested two mesomeric electronic transitions structures (A) and (B) producing a delocalized positive charges over the conjugated chromophoric group system of the dyes, Scheme (2).

3. The electronic visible absorption spectra of the examined cyanine dyes (5b) and (7b) in pure solvents having different polarities (solvatochromism) underwent displacements to give positive solvatochromism (occurrence of a bathochromic shift with increasing solvent polarity) and/or negative solvatochromism (occurance of a hypsochromic shift with increasing solvent polarity) depending upon the following factors:

a. Increasing and/or decreasing the polarity (dielectric constant) of the solvent (General solvent effect).

b. Hydrogen bond and/or molecular complex formation between the solute (dyes molecules) and the solvent used (specific solvent effect).

4. The electronic visible absorption spectra of the monomethine (5b) and trimethine (7b) cyanine dyes in aqueous universal buffer solutions having varied pH values (halochromism) underwent displacements to give hypsochromic shifted and lower intensity bands in the lower pH media (acidic media) due to the protonated and/or colourles structures of the dyes in this media. Inversely, the bands of these dyes are intensified and bathochromically shifted in high pH media (basic media) due to the deprotonated and/or coloured structures of the dyes in this media.

4. Experimental

4.1. General:

All the melting points of the prepared compounds are measured using Electrothermal 15V, 45W 1 A9100 melting pointapparatus (Chemistry, Faculty of Science, Aswan University, Aswan, Egypt) and are uncorrected. Elemental analysis was carried out at the Microanalytical Center of Cairo University by an automatic analyzer (Vario EL III Germany). Infrared spectra were measured with a FT-IR (4100 Jasco, Japan), Cairo University. ^{1}HNMR spectra were accomplished using Varian Gemini-300 MHz NMR Spectrometer (Cairo University). Mass Spectroscopy was recorded on Mass 1: GC2010 Shimadzu Spectrometer (Cairo University). Electronic visible absorption spectra were carried out on visible spectrophotometer spectra 24 RS Labomed, INC (Chemistry Department, Faculty of Science, Aswan University, Aswan, Egypt).

4.2-Synthesis:

4.2-1-Synthesis of 4-methyl-2-phenyl-benzo[(2,3-b)benzoxazine; (2', 3'-b')furo(3,2-d)pyrazole]-5,12-dione (3).

Equimolar ratios of 3,4-dichloro-benzo[b]-phenoxazine-2,5-dione (1) (0.01 mol, 2.8 gm) and 3-methyl-1-phenyl-5-pyrazolone (2) (0.01 mol, 1.7 gm) were dissolved in pyridine (50 ml). The reaction mixture was heated under reflux for (6-8 hrs) until the mixture attained a permanent brown colour. It was filtered off while hot to remove any impurities, concentrated, then poured in ice water mixture with continuous shaking. The precipitated compound was filtered, washed with cold water, air dried, collected and crystallized from ethanol. The data are reported in Table 1.

4.2-2-Synthesis of 3-ethyl-4-methyl-5,12-dione-2-phenyl-benzo[(2,3-b)benzoxazine;(2',3'-b')furo(3,2-d)pyrazolium]iodide quaternary salt (4).

Apure crystallized sample of (3) (0.04 mol, 1.5 gm) was suspended in excess of iodoethane (30 ml) and heated gently under reflux at low temperature (40-60°C) for 1hr. The solvent was evaporated and the residue was collected and crystallized from ethanol. See data in Table 1.

4.2-3-Synthesis of 3-ethyl-5,12-dione-2-phenyl-benzo[(2,3-b)benzoxazine;(2',3'-b')furo(3,2-d)pyrazole]-4[4(1)]-monomethine cyanine dyes (5a-c).

A mixture of compound (4) (0.01 mol, 0.5 gm) and iodoethane quaternary salts (0.01 mol) of pyridine (0.2 gm), quinoline (0.3 gm), or isoquinoline (0.3 gm) was refluxed in ethanol (50 ml) containing piperidine (3-5 drops) for 6-8 hrs. The reaction mixture, which changed from brown to red colour (for 5a), and/or deep red colour (for 5b, c) during the refluxing time, was filtered off while hot to remove any impurities, concentrated, cooled and precipitated by adding cold water. The precipitated products were collected and crystallized from ethanol. The relevent data are given in Table 1.

4.2-4. Synthesis of 3-ethyl-4(1,1'-diethoxyethyl)-5,12-dione-2-phenyl - benzo[(2,3-b)benzoxazine; (2',3'-b')furo(3,2-d)pyrazolium] iodide quaternary salt as intermediate compound (6).

This intermediate compound (6) was synthesized by refluxing of the quaternary salt compound (4) (0.04 mol, 2.4 gm) with triethylorthoformate (0.04 mol, 0.8 ml) in acetic anhydride (50 ml) for 3-5 hrs. The dark brown mixture was filtered on hot to remove any impurities, concentrated and precipitated by cold water. The separated intermediate compound was filtered, washed with water and crystallized from ethanol. The results are registered in Table 1.

4.2-5. Synthesis of 3-ethyl-5,12-dione-2-phenyl-benzo[(2,3-b)benzoxazine;(2',3'-b')furo(3,2-d)pyrazole]-4[2(4)]-trimethine cyanine dyes (7a-c).

A mixture of the intermediate compounds (6) (0.01 mol, 0.6 gm) and N-ethyl α-picolinium iodide quaternary salt (0.01 mol, 0.25 gm), N-ethyl quinaldinium iodide quaternary salt (0.01 mol, 0.3 gm) or N-ethyl γ-picolinium iodide quaternary salt (0.01 mol, 0.25 gm) were heated under reflux in ethanol (50 ml) containing piperidine (3-5 drops) for 6-8 hrs. The colour of the reaction mixture attained violet (for 7a), deep violet (for 7b) and violet (for 7c) at the end of the refluxing time. It was filtered off on hot, concentrated and precipitated by adding cold water. The separated cyanines were filtered, washed with cold water and crystallized from ethanol. The results are listed in Table 1.

4.3. Absorption spectral behavior in 95 % ethanol:

The electronic visible absorption spectra of the prepared cyanine dyes were examined in 95 % ethanol solution and recorded using 1Cm Qz cell in visible spectrophotometer, spectra 24 RS Labomed, INC. A stock solution ($1x10^{-3}$M) of the dyes was prepared and diluted to a suitable volume in order to obtain the desired lower concentrations. The spectra were recorded immediately to eliminate as much as possible the effect of time.

4.4. Absorption spectral behavior in pure solvents and/or in aqueous universal buffer solutions:

The electronic visible absorption spectra of some selected synthesized cyanine dyes were investigated in pure organic solvents of spectroscopic grade (Shindy et al., 2014; Shindy et al., 2014a) and different polarities and/or in aqueous universal buffer solutions of varying pH values and recorded using 1cm quartz cell in Vis spectrophotometer spectra 24 RS Labomed, INC. A stock solution (1 x 10-3M) of the dyes was prepared and diluted to a suitable volume using the suitable solvent and/or the buffer solution to obtain the required lower concentrations. The spectra were recorded immediately to eliminate as much as possible the effect of time.

5. Conflict of interest

There is no conflict of interest.

6. Acknowledgement

We are thankful to the Chemistry department, Faculty of Science, Aswan University, Aswan, Egypt for supporting this work.

References

Achilefu et al., 2000 – *Achilefu S., Dorshow R.B., Bugaj J.E., Rajagopalan R.* (2000). Novel receptor-targeted fluorescent contrast agents for in vivo tumor imaging. *Invest Radiol,* 35 (8), pp. 479-485.

Arjona et al., 2016 – *Argona A., Stolte M., Wilerthner F.* (2016). Conformational switching of π-conjugated junctions from merocyanine to cyanine statesby solvent polarity. *Angewandte Chemie,* 55(7), 2470-2473.

Ashitate et al, 2016 – *Ashitate Y., Levitz A., Park M.H., Hyun H., Venugopal V., Park G., El Fakhri G., Henary M., Gioux S., Frangioni J. V. et al.* (2016). Endocrine-specific NIR fluorophores for adrenal gland targeting. *Chem. Commun.,* 52, 10305–10308.

Choi et al., 2013 – *Choi H.S., Gibbs S.L., Lee J.H., Kim S.H., Ashitate Y., Liu F.B. et al.* (2013). Targeted zwitterionic near-infrared fluorophores for improved optical imaging. *Nat Biotechnol,* 31 (2), pp. 148-153.

Choi, et al., 2011 – *Choi H.S., Nasr K., Alyabyev S., Feith D., Lee J.H., Kim S.H. et al.* (2011). Synthesis and in vivo fate of zwitterionic near-infrared fluorophores. *Angew Chem Int Ed,* 50 (28), pp. 6258-6263.

Dach, Daehne 1997 – *Dach G., Daehne S. (*1997). Second supplements to the 2nd edition of rodd's chemistry of carbon compounds, Vol. IV B. Elsevier Science B.V., Chapter 15, Cyanine dyes and related compounds (edited by Sainsbury, M.).

Dähne et al. 1998 – *Dahne S., Resch-Genger U., Wolfbeis O.S.* (1998). North Atlantic Treaty Organization. Scientific Affairs Division**.** Near-infrared dyes for high technology applications. Kluwer, Dordrecht; Boston.

Deligeorgiev et al., 1998 – *Deligeorgiev T.G., Zaneva D.A., Kim S.H., Sabnis R.W.* (1998)**.** Preparation of monomethine cyanine dyes for nucleic acid detection**.** *Dyes Pigments,* 37 (3), pp. 205-211.

Hamer, 1964 – *Hamer F.M.* (1964). The cyanine dyes and related compounds**.** Interscience Publishers, New York.

Haugland et al., 1969 – *Haugland R.P., Spence M.T.Z., Johnson I.D.* (1969)**.** Handbook of fluorescent probes and research chemicals**.** (6th ed.), Molecular Probes, Eugene, OR, USA (4849 Pitchford Ave., Eugene 97402).

Hyun et al., 2015 – *Hyun H., Owens E.A., Wada H., Levitz A., Park G., Park M.H., Frangioni J.V., Henary M., Choi H.S.* (2015). Cartilage-specific near-infrared fluorophores for biomedical imaging. *Angew. Chem. Int. Ed. Engl.,* 54, 8648-8652.

Licha et al., 2000 – *Licha K., Riefke B., Ntziachristos V., Becker A., Chance B., Semmler W.* (2000). Hydrophilic cyanine dyes as contrast agents for near-infrared tumor imaging: synthesis, photophysical properties and spectroscopic in vivo characterization. *Photochem Photobiol,* 72(3), pp. 392-398.

Musso, 1979 – *Musso H.* (1979). The pigments of fly agaric, Amanita muscaria. Tetrahedron, 35 (24), pp. 2843-2853.

Nakazumi, 2008 – *Nakazumi H.* (2008)**.** Organic colorants for laser disc optical data storage. *J Soc Dye Colour,* 104(3), pp. 121-125.

Reichardt**,** 1995 – *Reichardt C.* (1995)**.** Chiral polymethine dyes: a remarkable but forgotten conjugated pi system. *J Phys Org Chem,* 8 (12), pp. 761-773.

Rodríguez-Pérez et al., 2017 – *Rodriguez-Perez L., Villegas C., Herranz M.A., Delgado J.L., Martín, N.* (2017). Heptamethine Cyanine Dyes in the Design of Photoactive Carbon Nanomaterials. *ACS Omega,* 2(12): 9164–9170.

Sato et al., 2019 – *Sato Y., Yajima S., Taguchi A., Baba K., Nakagomi M., Aiba, Y., Nishizawa, S.* (2019). Trimethine cyanine dyes as deep-red fluorescent indicators with high selectivity to the internal loop of the bacterial A-site RNA. *Chem. Commun.,* 55, 3183-3186.

Schwechheimer et al., 2018 – *Schwechheimer C., Ronicke F., Schepersb, U., Wagenknecht, H.* (2018). A new structure–activity relationship for cyanine dyes to improve photostability and fluorescence properties for live cell imaging. *Chem. Sci.,* 9, 6557.

Shindy et al., 2014 – *Shindy H.A., El-Maghraby M.A., Eissa F.M.* (2014). Effects of Chemical structure, solvent and solution pH on the visible spectra of some new methine cyanine dyes. *European Journal of Chemistry,* 5(3), 451-456.

Shindy et al., 2014a – *Shindy H.A., El-Maghraby M.A., Eissa F.M.* (2014). Synthesis and Sprctral Properties of Novel Hemicyanine dyes. *Izv. AN. Ser. Khim,* 63(3), 707-715.

Shindy et al., 2019 – *Shindy H.A., El-Maghraby M.A., Goma M.M., Harb N.A.* (2019). Novel styryl and aza-styryl cyanine dyes: synthesis and spectral sensitization evaluation. *Chemistry International*, 5(2), 117-125.

Shindy, 2017 – *Shindy H.A.* (2017). Fundamentals in the Chemistry of Cyanine Dyes: A Review. *Dyes and Pigments,* 145, 505-513.

Shindy, 2018 – *Shindy H.A.* (2018). Structure and solvent effects on the electronic transitions of some novel furo/pyrazole cyanine dyes. *Dyes and Pigments,* 149, 783-788.

Soriano et al., 2015 – *Soriano E., Holder C., Levitz A., Henary M.* (2015). Benz[c,d]indolium-containing monomethine cyanine dyes: Synthesis and photophysical properties. *Molecules,* 21.

Wade, 1999 – *Wade Jr.L.G.* Organic. Chemistry. 4th Edn., Pearson Educ. (Prentice Hall, Upper Saddle River, New Jersy 07458, USA), 500-538.

Wade, 1999a – *Wade Jr.L.G.* Organic. Chemistry. 4th Edn., Pearson Educ. (Prentice Hall, Upper Saddle River, New Jersy 07458, USA), 544-604.

Warner et al., 1996 – *Warner I.M., Soper S.A., McGown L.B.* (1996)**.** Molecular fluorescence, phosphorescence, and chemiluminescence spectrometry**.** *Anal Chem,* 68 (12), pp. R73-R91.

Wyler, 1969 – *Wyler H.* (1969). Die Betalaine**.** *Chemie unserer Zeit,* 3 (5), pp. 146-151.

Wyler, 1969a – *Wyler H.* (1969). Das Experiment: Papierelektrophorese. *Chemie unserer Zeit,* 3 (4), pp. 111-115.

Xu et al., 2007 – *Xu Y.F., Liu Y., Qian, X.H.* (2007). Novel cyanine dyes as fluorescent pH sensors: PET, ICT mechanism or resonance effect? *J Photochem Photobiol A,* 190(1), pp. 1-8.

Appendix

Table 1. Characterization of the prepared compounds 3, 4, (5a-c), 6 and (7a-c)

Comp No	Nature of products			Molecular formula (M.Wt)	Analysis%						Absorption spectra in 95% ethanol	
	Colour	yield %	MP C°		Calculated			Found			λmax(nm)	ε_{max} (mol⁻¹.cm²)
					C	H	N	C	H	N		
3	Brown crystals	70	150	$C_{22}H_{13}N_3O_4$(383)	68.93	3.39	10.97	68.93	3.12	10.88	.....	.....
4	Dark brown crystal	64	145	$C_{24}H_{18}N_3O_4I$(539	50.7	3.17	7.39	50.56	3.11	7.24	.....	.....
5a	Red	60	144	$C_{31}H_{25}N_4O_4I$(644	57.76	3.88	8.7	57.66	3.76	8.59	410, 440	12360, 13390
5b	Deep red	64	155	$C_{35}H_{27}N_4O_4I$(694	60.52	3.89	8.07	60.45	3.77	8.02	440, 460	14760, 14990
5c	Deep red	62	165	$C_{35}H_{27}N_4O_4I$(694	60.52	3.89	8.07	60.49	3.86	8.01	420, 450	16180, 14100
6	Dark brown crystal	59	160	$C_{29}H_{28}N_3O_6I$(641	51.94	4.18	6.27	51.44	4.13	6.22	.....	.....
7a	Violet	66	163	$C_{33}H_{27}N_4O_4I$(670	59.1	4.03	8.36	59.05	4.01	8.33	410, 440, 570	10590, 11590, 6400
7b	Deep violet	69	186	$C_{37}H_{29}N_4O_4I$(720	61.67	4.03	7.78	61.63	4.02	7.72	460, 590, 650	15390, 8780, 5000
7c	Violet	67	178	$C_{33}H_{27}N_4O_4I$(670	59.1	4.03	8.36	59.02	4.01	8.31	420, 450, 580	13080, 14090, 7350

Table 2. IR and ^{1}H NMR (Mass) Spectral Data of the Prepared Compounds (3), (4), (5b), (6) and (7b)

Comp. No.	IR Spectrum (KBr, Cm^{-1})	^{1}H NMR Spectrum (DMSO, δ); & (Mass data).
3	689, 755 (monosubstituted phenyl). 870 (o.disubstituted phenyl). 1485 (C=N). 1597 (C=C). 1712 (C=O quinone). 3423 (NH).	2.1 (m, 3H, CH_3 of position 4). 3.5 (b, 1H, NH). 6.8-9.25 (m, 9H, aromatic). M^{+1}: 383.88
4	619, 686 (monosubstituted phenyl). 1116 (C—O—C cyclic). 1363 (C—N). 1489 (C=N). 1594 (C=C). 1712 (C=O quinone). 2924 (quaternary salt). 3428 (NH).	1.2 (m, 3H, CH_3 of position 3). 1.6 (s, 3H, CH_3 of position 4). 2.2 (m, 2H, CH_2 of position 3). 3.5 (b, 1H, NH). 6.8-9.3 (m, 9H, aromatic). M^{+1}: 539.90
5b	618, 688 (monosubstituted phenyl). 755 (o.disubstituted phenyl). 1115 (C—O—C cyclic). 1381 (C—N). 1490 (C=N). 1627 (C=C). 2924 (quaternary salt). 3441 (NH).	1.3 (m, 3H, CH_3 of position 3). 1.6 (m, 3H, CH_3 of N-quinolinium). 2.1 (b, 4H, $2CH_2$ of position 3 and N-quinolinium). 3.4 (m, 1H, NH). 5.15 (s, 1H, —CH=). 7.1-9.6 (m, 15H, aromatic + heterocyclic).
6	688, 755 (monosubstituted phenyl). 838 (o.disubstituted phenyl). 1366 (C—N). 1491 (C=N). 1616 (C=C). 1711 (C=O quinone). 2925 (quaternary salt). 3437 (NH).	0.9 (b, 3H, CH_3 of position 3) 1.1-1.6 (m, 7H, $2CH_3$ of diethoxyethyl + 1H, — CH< of diethoxyethyl). 0.9-2.2 (m, 8H, CH_2 of position 3 + $3CH_2$ of diethoxyethyl). 3.35 (b, 1H, NH). 7-9.2 (m, 9H, aromatic). M^{+} : 641.15
7b	617, 688 (monosubstituted phenyl). 755 (o.disubstituted phenyl). 1116, 1157 (C—O—C cyclic). 1363 (C—N). 1494 (C=N). 1626, 1599 (C=C). 1711 (C=O quinone). 2922, 2845 (quaternary salt). 3437 (NH).	0.9-1.4 (m, 3H, CH_3 of position 3). 1.5-1.8 (m, 3H, CH_3 of N-quinolinium). 1.9-2.4 (b, 4H, $2CH_2$ of position 3 and N-quinolinium). 3.4 (s, 1H, NH). 6.8-8.5 (m, 18H, aromatic + heterocyclic + 3 —CH=).

Table 3. Visible absotption spectra of the dyes (5b and 7b) in pure solvents having different polarities

Solvent / Dye No.	H_2O		EtOH		DMF		$CHCl_3$		CCl_4		Dioxane	
	λ_{max} (nm)	ε_{max} (mole^{-1}cm^2)	λ_{max} (nm)	ε_{max} (mole^{-1}cm^2)	λ_{max} (nm)	ε_{max} (mole^{-1}cm^2)	λ_{max} (nm)	ε_{max} (mole^{-1}cm^2)	λ_{max} (nm)	ε_{max} (mole^{-1}cm^2)	λ_{max} (nm)	ε_{max} (mole^{-1}cm^2)
5b	420 450	14040 13000	440 460	14760 14990	480 500	21000 21500	440 470	15950 15870	460 480	11860 12330	470 490	17000 16680
7b	440 480 580 640	14160 14620 7290 4530	460 590 650	15390 8780 5000	490 520 620 690	20040 19590 11910 8100	470 600 660	14820 10300 6100	480 510 610 670	17900 17210 10160 7011	480 500 610 680	18630 18360 10160 4510

Table 4. Visible absorption spectra of the dyes (5b and 7b) in aqueous universal buffer solutions

Comp. No.	Universal Buffers							
	1.99		2.99		4.30		6.87	
	λ_{max} (nm)	ε_{max} (mol^{-1}cm^2)	λ_{max} (nm)	ε_{max} (mol^{-1}cm^2)	λ_{max} (nm)	ε_{max} (mol^{-1}cm^2)	λ_{max} (nm)	ε_{max} (mol^{-1}cm^2)
5b	415 440 578	9200 11280 6310	416 450 580	9400 10780 6320	417 452 582	9500 10900 6500	418 454 583	9700 10950 7300
7b	420 450 560 620	9180 9960 6570 3360	430 470 570 630	9800 8690 6690 3380	422 453 580 640	9181 9964 6890 3380	425 440 580 642	9730 11720 6891 3590

Table 4. Continue. Visible absorption spectra of the dyes (5b and 7b) in aqueous universal buffer solutions

Comp. No.	Universal Buffers							
	7.96		8.91		10.55		12.04	
	λ_{max} (nm)	ε_{max} (mol^{-1}cm^2)	λ_{max} (nm)	ε_{max} (mol^{-1}cm^2)	λ_{max} (nm)	ε_{max} (mol^{-1}cm^2)	λ_{max} (nm)	ε_{max} (mol^{-1}cm^2)
5b	419 457 585	10000 10780 8500	420 440 586	13270 13100 9500	422 445 587	13500 13300 9900	424 450 589	13270 13750 11900
7b	430 460 580 648	9800 10390 6890 4000	440 460 590 650	11720 11760 7360 4200	430 450 591 652	12140 12610 7380 4400	430 460 593 660	12142 13250 84200 5000

Table 5. The variation of absorbance with pH at fixed λ for the dyes (5b and 7b) in aqueous universal buffer solutions

	Compound Number Absorpance at fixed λ	
pH	5b λ=580 (nm)	7b λ=650 (nm)
1.99	0.63	0.273
2.99	0.7	0.224
4.30	0.75	0.226
6.87	0.8	0.295
7.96	0.9	0.299
8.91	1	0.37
10.55	1.05	0.43
12.04	1.2	0.48
Pka	8.7	8.9 6.1

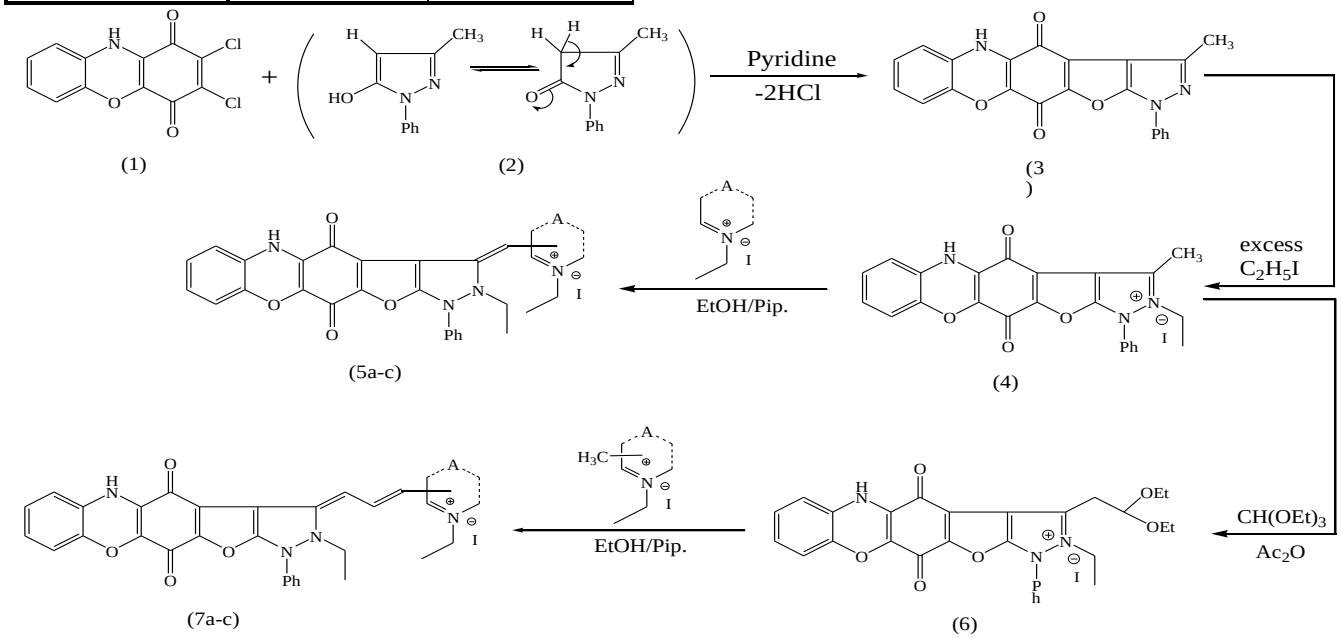

Scheme (1)
Synthesis Strategy of the prepared compounds (3), (4), (5a-c), (6) and (7a-c).

Substituents in scheme (1):

(5a-c): A = 1-ethyl pyridinium-4-yl salt (a), 1-ethyl quinolinium-4-yl salt (b), 2-ethyl isoquinolinium-1-yl salt (c).

(7a-c): A = 1-ethyl pyridinium-2-yl salt (a), 1-ethyl quinolinium-2-yl salt (b), 1-ethyl pyridinium-4-yl salt (c).

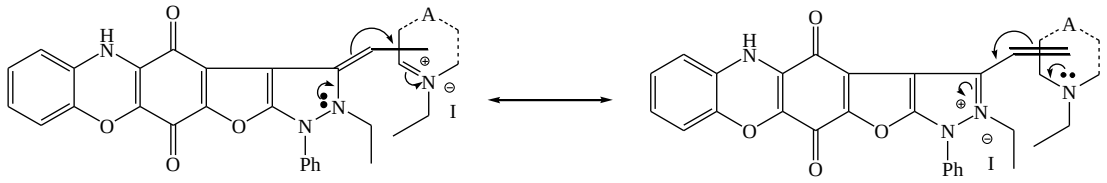

(A) (B)

(5a-c)

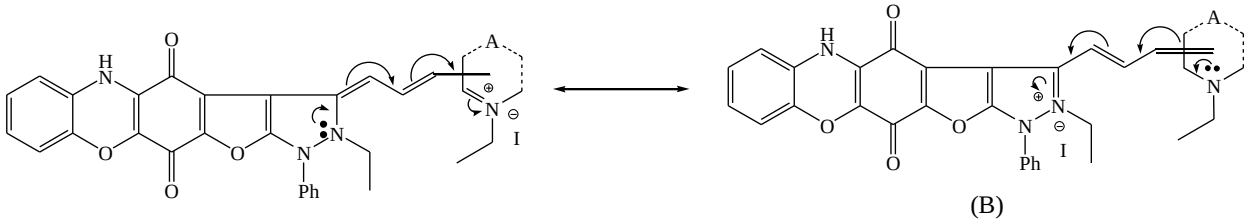

(A) (B)

(7a-c)

Scheme (2)

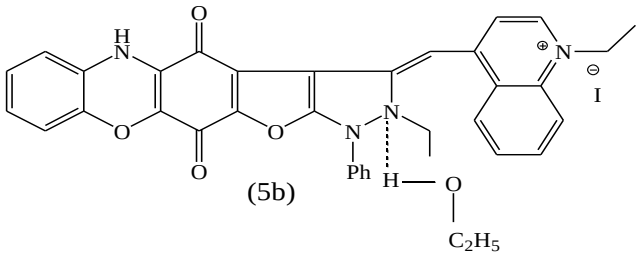

(5b)

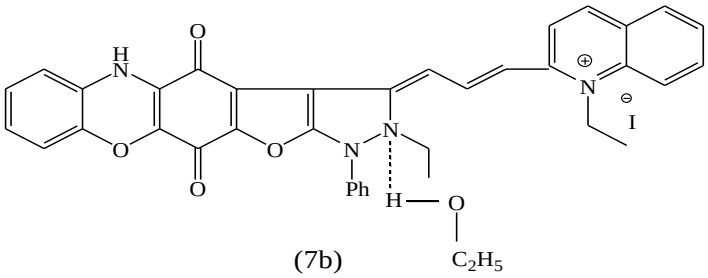

(7b)

c). **(A)**

Scheme (3)

Colour intensity and the electronic charge transfer pathways illustration of the synthesized monomethine cyanine dyes (5a-c) and trimethine cyanine dyes (7a-c). Hydrogen bond formation between the monomethine cyanine dye (5b), trimethine cyanine dye (7b) and ethanol molecules (specific solvent effect).

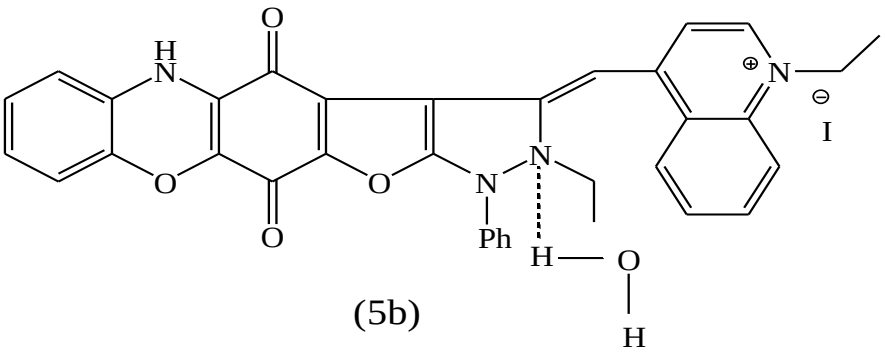

(5b)

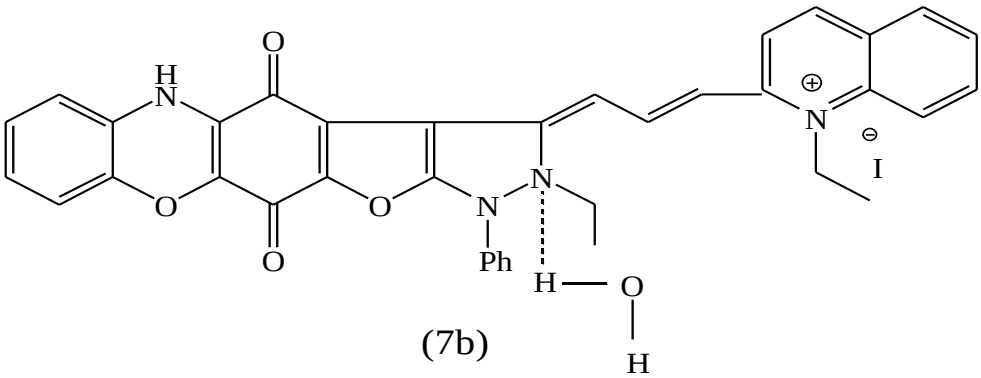

(7b)

(B)

Scheme (3)

Hydrogen bond formation between the monomethine cyanine dye (5b), trimethine cyanine dye (7b) and water molecules (specific solvent effect).

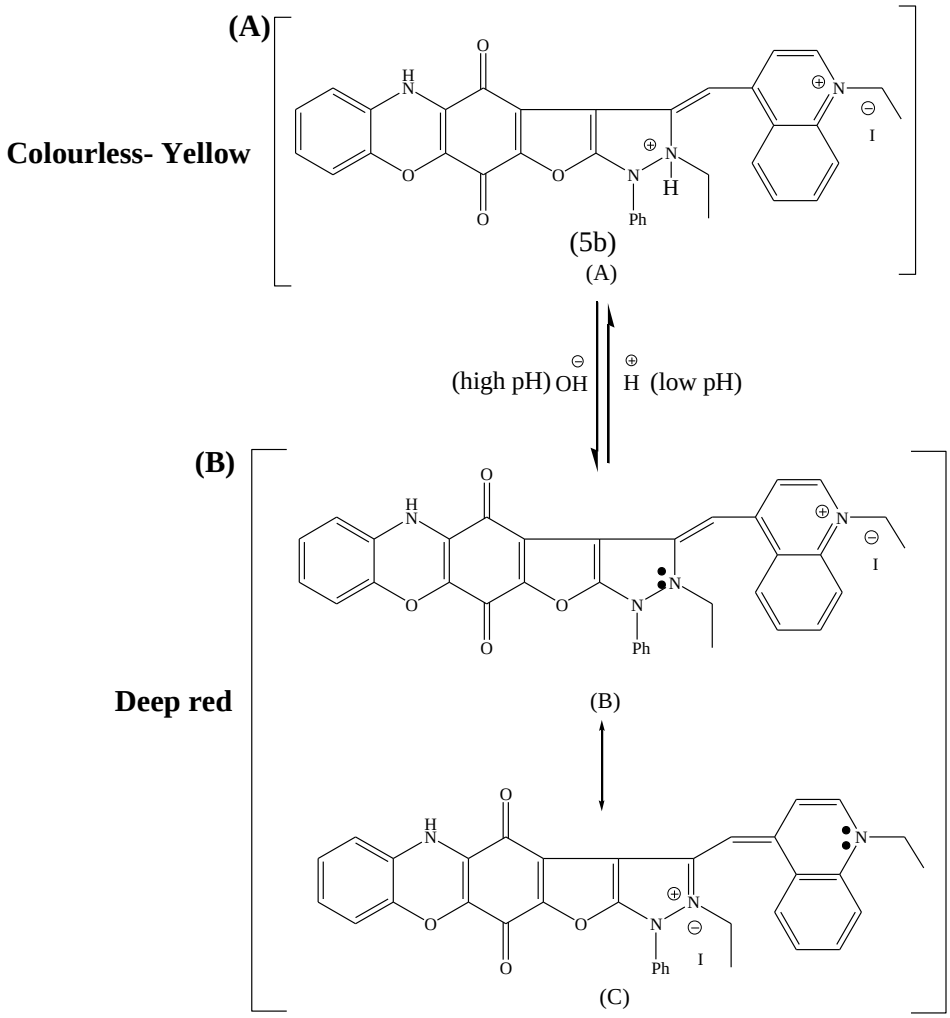

Effects of pH media on the colour change of the monomethine cyanine dye (5b)

Decolourization (protonation) and colourization (deprotonation) of the monomethine cyanine dye (5b) in acid and base media, respectively (acido-basic equilibrium).
Scheme (4)

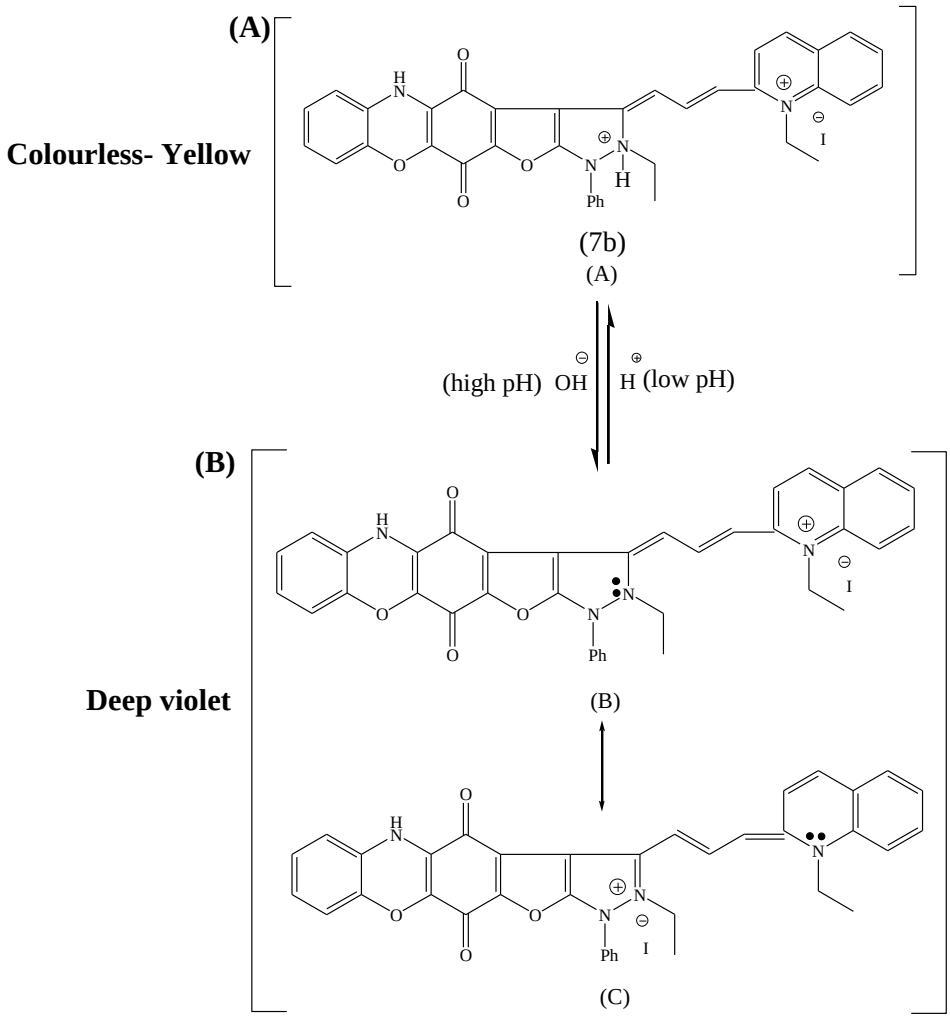

Effects of pH media on the colour change of the trimethine cyanine dye (7b)

Decolourization (protonation) and colourization (deprotonation) of the trimethine cyanine dye (7b) in acid and base media, respectively (acido-basic equilibrium).
Scheme (4) Continue

Published in the Slovak Republic
European Journal of Molecular Biotechnology
Has been issued since 2013.
E-ISSN: 2409-1332
2019, 7(1): 40-46

DOI: 10.13187/ejmb.2019.1.40
www.ejournal8.com

Toward Human Health-Promoting Food Plants: Perspectives of Marker-Assisted Breeding of Anthocyanin-Rich Lettuce

Valery G. Zaitsev [a, b, *], Regina Yu. Ivashchenko [a], Darya A. Kurkina [a], Anna S. Popova [b]

[a] Federal Research Centre of Agroecology, Complex Melioration, and Forest Reclamations RAS, Volgograd, Russian Federation
[b] Volgograd State University, Volgograd, Russian Federation

Abstract

Development and growing of plant cultivars with elevated content of health beneficial nutrients could improve the public human health. The aim of this study was to review the state of the art in use of molecular markers to produce anthocyanin-rich varieties of lettuce (*Lactuca sativa* L.). Link between anthocyanins production and their proved effect on the health was discussed. Although anthocyanin-dependent red colour of lettuce has been used in breeding for years the metabolic markers are not high-quality for noted purpose. Use of molecular markers can improve results of the breeding. Known and perspective DNA-based molecular markers were shown in this mini-review.

Keywords: lettuce, marker-assisted breeding, human health, molecular marker, anthocyanins, antioxidants, genetic profiling, single nucleotide polymorphisms, metabolic markers.

1. Introduction

Quality and composition of food is extremely important for human health. At least 22 % of all death in adult population all over the world are resulted from action of dietary risk factors (GBD 2017 Diet Collaborators, 2019). Sufficient daily intake of vegetables (optimal level is 290–430 g per day) have benefits for health. On the other hand, increased nutrients content in vegetables can improve health conditions even in the case of low vegetables consumption that recognized as one of five strongest dietary risk factors. Nutrient composition of vegetables is very variable and determined by genetic and environmental factors both. Therefore, elevated production of human health beneficial nutrients is important goal in breeding of cultivated plants (Hansson et al., 2018).

Anthocyanins, a subgroup of flavonoids, are plant secondary metabolites with proven benefits for human health (Khoo et al., 2017; Yang et al., 2017; Rees et al., 2018). However, concentration of anthocyanins in plant tissues can vary dramatically and is controlled by multiple exogenous stimuli like light intensity, salt concentration, humidity, temperature and so on (Liu et al., 2018). Specified variability is especially meaningful in leafy vegetables that require development of new cultivars with sustained high production of anthocyanins.

The aim of this study was to review the state of the art in use of molecular markers to produce anthocyanin-rich varieties of lettuce (*Lactuca sativa* L.).

* Corresponding author
E-mail addresses: valeryzaitsev@gmail.com (V.G. Zaitsev), Regina.Niki5@yandex.ru (R.Yu. Ivashchenko), rotor3480@gmail.com (D.A. Kurkina), anna1996popova@yandex.ru (A.S. Popova)

2. Anthocyanins

2.1. Structure and distribution in nature

Anthocyanins are particular members of the flavonoid family among plant phenols. Anthocyanins are glycosilated polyphenolic compounds found in a lot of plants and giving them various colours – from orange and red to blue and purple. Plants contains little amounts of aglyconic forms of anthocyanins called antocyanidins as anthocyanidins are precursors in biosynthesis of anthocyanins. Both anthocyanidins and antocyanins are positive charged and coloured under physiological conditions but only glycosylated compounds can be accumulated into vacuoles (Castañeda-Ovando et al., 2009). More than 700 anthocyanins have been found in plants to the date (Smeriglio et al., 2016; Santos-Buelga, González-Paramás, 2019). Glycosides of cyanidin, pelargonin, delphinidin, peonidin, petunidin and malvidin are most common anthocyanins in plants (Khoo et al., 2017).

Anthocyanins play multiple physiological roles in plants. Firstly, they colourize flowers to attract pollinators and edible fruits to improve the chances of seed dissemination by animals eating fruits, therefore anthocyanins are important for plant reproduction (Pervaiz et al., 2017). Secondary, anthocyanins are involved in physiological response to various biotic and abiotic stresses. Influence of many dangerous factors including drought, heavy metals, pathogenic viruses and microbes invasion can be diminished by anthocyanins. Moreover, anthocyanidins have antioxidative properties and effectively scavenge free radicals and reactive oxygen species produced in particular during UV and light-induced photodamage (Gould, 2004).

Contents of anthocyanins in edible plants vary widely – from less than 10 μg/g to about 14 mg/g (Santos-Buelga, González-Paramás, 2019). Common food sources of anthocyanidins are brightly-coloured fruits and berries containing cyanidin derivatives like apple, plum, cherry, blackberry, raspberry, strawberry (Andersen, Jordheim, 2013). Blackberry, blueberry, black currant and chokeberry have the highest concentration of anthocyanins among edible berries and (Santos-Buelga, González-Paramás, 2019) and black carrot, red cabbage, black soybeans, purple batat and purple potato among vegetables (Khoo et al., 2017).

2.2. Effect on human health

Some human health beneficial effects of anthocyanins were proved and a significantly larger number of biological activities were tested in experimental studies and clinical trials (Smeriglio et al., 2016; Khoo et al., 2017). Li et al. summarized results of clinical trials and noted anthocyanins from fruits and vegetables can decrease risk of development or progression of some cancers including tumours of breast, prostate, liver, colon, lungs, cervix as well as metastatic melanoma (Li et al., 2017). Antiinflammatory properties, neuroprotective action of anthocyanins and their benefits for cognition and memory were discussed too (Mulabagal et al., 2010; Li et al., 2017).

Some clinical trials showed attenuating effects of anthocyanins on human cardiovascular risk factors including elevated blood pressure and dysfunction of vessel endothelium but other studies exhibited controversial results (Rees et al., 2018). Possible mechanisms of action include decline of low density lipoproteins oxidation, elevation of blood antioxidant capacity, and attenuation of dyslipidemia (Reis et al., 2016). There are evidences of antiobesity and antidiabetic effects of anthocyanins from experimental and clinical studies (Azzini et al., 2017; Lee et al., 2017; Yang et al., 2017).

Therefore, anthocyanins have multiple positive effects on human health and long-term consumption of vegetable and fruits containing more anthocyanins could prevent some cases of disease development without use of pharmaceuticals.

2.3. Anthocyanins in lettuce

Lettuce (Lactuca sativa L.) is one of the widely used leaf vegetables and is a member of the Asteraceae family (Anilakumar et al., 2017). Lettuce has short vegetation period and can be easy grown in field or soil-based greenhouse as well as by use of hydroponic, aeroponic or vermiponic systems (Barbosa et al., 2015; Bartzas et al., 2015). There are green and red varieties of lettuce and the last ones can accumulate anthocyanins in leaves and stem. Anthocyanins content in lettuce can vary very widely: from {negligible or trace amounts} 1.9 μg/g fresh weight in green varieties (Mampholo et al., 2016) to 874.4 μg/g dry weight in red or purple ones (Gazula et al., 2007). Different species of plants contain limited number anthocyanins although chemical diversity of

them is great (Chaves-Silva et al., 2018). Glucosides of cyanidin and peonidin were detected as major anthocyanins in Lactuca sativa.

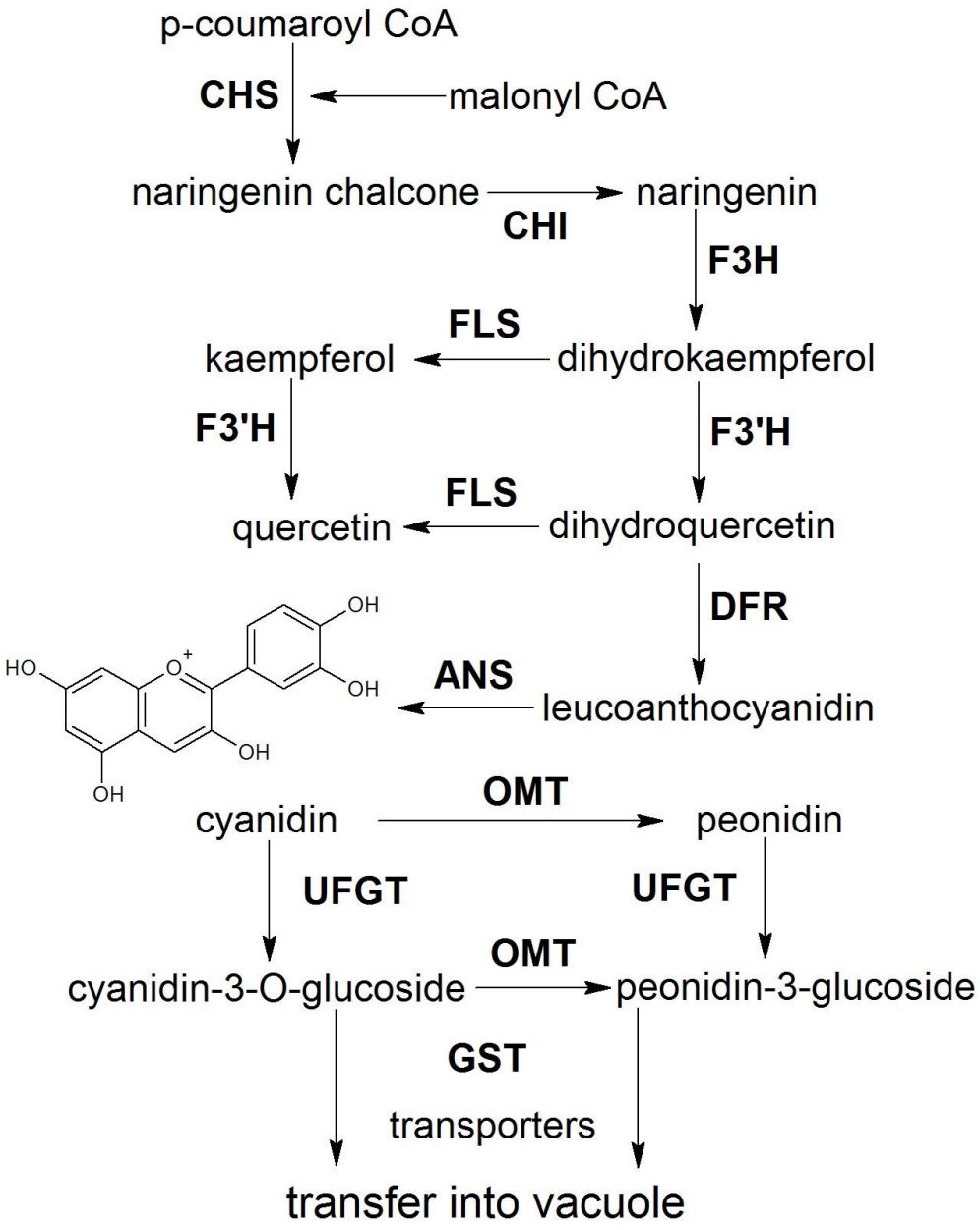

Fig. 1. Metabolic pathway of flavonoids anf antocyanins biosynthesis in lettuce.
See abbreviation in the text

Biosynthesis of antocyanins in lettuce (Figure 1) needs sequential formation of some flavonoids as precursors (Winkel-Shirley, 2001; Pervaiz et al., 2017). Consequently, this biochemical pathway requires the participation of following enzymes noted on Figure 1: chalcone synthase(CHS, EC: 2.3.1.74), chalcone isomerase (CHI, EC: 5.5.1.6), naringenin 3-dioxygenase or flavonone 3-hydroxylase (F3H, EC: 1.14.11.9), flavonol synthase (FLS, EC: 1.14.20.6), flavonoid 3'-monooxygenese or flavonoid 3'-hydroxylase (F3'H, EC: 1.14.14.82), dihydroflavonol 4-reductase (DFR, EC: 1.1.1.219), anthocyanidin synthase (ANS, EC: 1.14.20.4, also known as leucocyanidin oxygenase or leucoanthocyanidin dioxygenase - LDOX), anthocyanidin 3-O-glucosyltransferase or flavonoid 3-O-glycosyltransferase (3GT or UFGT, EC: 2.4.1.115) and glutathione S-transferase (GST, EC 2.5.1.18). Enzymes from CHS to F3'H are components of flavonoid metabolism pathway and - excluding FLS – involved in synthesis of dihydroquercetin, a immediate precursor of lettuce anthocyanidins. DHF and ANS produces cyanidin, a principal antocyanidin of lettuce (Winkel-

Shirley, 2001; Pervaiz et al., 2017). Glycosylation of anthocyanidins to anthocyanins is necessary for following their tranclocation into vacuoles with the assistance of GST (or GST-like proteins) and multi-drug resistance-like proteins from ABC transporter family (Tanaka et al., 2008). Cyanidin and cyanidin 3-glusoside can be transformed in peonidin and peonidin 3-glucoside respectively by unidentified O-methyltransferase(s) (OMT) possibly like anthocyanidin OMT from other plants (Provenzano et al., 2014).

Rate of the anthocyanins formation is highly variable between various cultivars of lettuce, between different plants of the same cultivar and even in individual plant during its development since production of anthocyanins plays key role in plant adaptation especially for adaptation to local ecosystems (Mouradov, Spangenberg, 2014). Therefore, anthocyanins biosynthesis rate is closely controlled by multiple environmental factors including intensity and spectral properties of light, temperature, humidity, presence of various substances in soil and air, microbial or viral infections. These factors can influence both total concentration and composition of anthocyanins in lettuce (Becker et al., 2014; Brücková et al., 2016; Kitazaki et al., 2018).

3. Marker-assisted breeding of lettuce for anthocyanin enrichment

Once anthocyanins give lettuce red colouration the colour of leaves and stem have been using in lettuce breeding for years. Typically, lettuce colouration can be estimated visually (Sochor et al., 2019). It is very subjective test. There have been attempts to improve measurement of anthocyanins content by use of biochemical assays (Şakar et al., 2008; Volden et al., 2009), reflective photometry (Gazula et al., 2007; Volden et al., 2009) or digital image analysis (Yang et al., 2016). Whatever the case, metabolic profiling/phenotyping in case of anthocyanins can give strong bias due to production of the anthocyanins is markedly dependent upon a lot of environmental factors. Differences in anthocyanins content in plant of the same cultivar can be up 1.5-fold in the same year and larger than 2-fold between different years (Gazula et al., 2007). Use of expressed mRNA or proteins as markers can be inappropriate for the same reasons. Use of DNA-based molecular markers can improve results of the marker-assisted breeding (Collard, Mackill, 2008; Nadeem et al., 2018).

Unfortunately, there are just a few studies for screening of DNA-based molecular markers associated with anthocyanins production in lettuce. Zhang et al. (Zhang et al., 2017) used transcriptome analysis of 163 cultivars to find candidate genes associated with flavonoid biosynthesis regulation. In theory, any of genes involved in biosynthesis of flavonoids including anthocyanins (see section 1.3) could be related with forming with anthocyanin-dependent red colouring in lettuce plants. However, Zhang et al. found only genes for ANS and GST had higher level of expression in red lettuce comparing to green lettuce. Additionally, expression levels of genes MYB113 (encoding one of MYB family transcription factors), bHLH42 (encoding transcription factor TT8) and LG1_162414 (encoding RING/U-box superfamily protein) were related with anthocyanins positively. Their products are regulatory proteins probably involved in plant adaptation processes. Only gene encoding cinnamyl-alcohol dehydrogenase (CAD) correlated to red colouration of lettuce leaves negatively. Nevertheless, statistically identified anthocyanin synthesis up-regulation single nucleotide polymorphisms (SNPs) were partially related to candidate genes above. In fact, only SNP in position 125530709 on chromosome LG1 was inside LG1_162414 gene the expression of which correlated with anthocyanin accumulation. Other 8 SNPs located on chromosomes LG3, LG4 and LG5 were not associated with any of the candidate genes (Zhang et al., 2017).

Genome-wide analysis of 298 lines of lettuce allowed to find 4 SNPs associated with anthocyanins levels. Particularly noteworthy was the fact that all found SNPs were related to content of anthocyanins in leaves but only 2 of them were additionally associated with anthocyanins concentration in stem (Kwon et al., 2013). Five cultivars of cultivated lettuce and 60 recombinant inbred line generated from a cross between cultivated lettuce (*L. sativa*) and wild *L. serriola* were used for search of quantitative trait loci (QTLs) related to antioxidant status. Three QTLs associated with anthocyanins production and red colouring were found on chromosome LG3. Two QTLs were observed inside genes of MYB family transcription factor: production of anthocyanin pigment 2 (PAP2) protein also known as MYB90 and MYB114. One more QTL was identified inside gene for F3H, enzyme involved in flavonoid biosynthesis. All three QTLs can be used as DNA-based molecular markers in cultivated *L. sativa* and wild *L. serriola* both (Damerum

et al., 2015). MYB transcription factor are well known as regulator of the dihydroflavonols to anthocyanidins conversion (Allan et al., 2008).

In general, use of wild species of genus *Lactuca* can give additional benefits in anthocyanin-rich lettuce breeding for two main reasons: (1) various *Lactuca* species can be hybridizied with cultivated lettuce relative easy, and (2) expression levels of some anthocyanin-related markers in wild *Lactuca spp*. are higher than in *L. sativa* (Damerum et al., 2015).

4. Conclusion

1. High content of the anthicyanins in edible plants can attenuate some disease and improve the public human health.
2. Use of metabolic, protein-based and mRNA-based markers in breeding of anthocyanin-rich lettuce cultivars can lead to limited success due to large variations in anthocyanins content under the effect of multiple epigenetic factors.
3. Use of DNA-based molecular markers is more appropriate.
4. Three QTLs and 13 SNPs associated with anthocyanin production in Lactuca sativa have been identified.
5. Hybridization of cultivated lettuce with wild *Lactuca spp*. can give additional benefits for anthocyanin-rich cultivars molecular selection.

References

Allan et al., 2008 – *Allan A.C., Hellens R.P., Laing W.A.* (2008). MYB transcription factors that colour our fruit. *Trends Plant Sci.* 13(3): 99-102. DOI: 10.1016/j.tplants.2007.11.012

Andersen, Jordheim, 2013 – *Andersen Ø.M., Jordheim M.* (2013). Basic Anthocyanin Chemistry and Dietary Source. In book: Anthocyanins in Health and Disease. Edoted by Wallace T.C., Giusti M.M. CRC Press. pp. 13-90.

Anilakumar et al., 2017 – *Anilakumar K.R., Harsha S.N., Mallesha, Sharma R.K.* (2017). Lettuce: A Promising Leafy Vegetable with Functional Properties. *Defence Life Sci. J.,* 2(2): 178-185. DOI: 10.14429/dlsj.2.11357

Azzini et al., 2017 – *Azzini E., Giacometti J., Russo G.L.* (2017). Antiobesity Effects of Anthocyanins in Preclinical and Clinical Studies. *Oxid. Med. Cell Longev.* 2017: 2740364. DOI: 10.1155/2017/2740364

Barbosa et al., 2015 - *Barbosa G.L., Gadelha F.D., Kublik N., et al.* (2015). Comparison of Land, Water, and Energy Requirements of Lettuce Grown Using Hydroponic vs. Conventional Agricultural Methods. *Int. J. Environ. Res. Public Health.* 12(6): 6879-6891. DOI: 10.3390/ijerph120606879

Bartzas et al., 2015 – *Bartzas G., Zaharaki D., Komnitsas K.* (2015). Life cycle assessment of open field and greenhouse cultivation of lettuce and barley. *Inf. Processing Agricult.*, 2(3-4): 191-207. DOI: 10.1016/j.inpa.2015.10.001

Becker et al., 2014 – *Becker C., Klaering H.P., Kroh L.W., Krumbein A.* (2014). Cool-cultivated red leaf lettuce accumulates cyanidin-3-O-(6″-O-malonyl)-glucoside and caffeoylmalic acid. *Food Chem.,* 146: 404-411. DOI: 10.1016/j.foodchem.2013.09.061

Brücková et al., 2016 – *Brücková K., Sytar O., Ţivčák M. et al.* (2016). The effect of growth conditions on flavonols and anthocyanins accumulation in green and red lettuce. *J. Central Eur. Agricult.*, 17(4): 986-997. DOI: 10.5513/JCEA01/17.4.1802

Castañeda-Ovando et al., 2009 – *Castañeda-Ovando A., de Lourdes Pacheco-Hernández M., Páez-Hernández E. et al.* (2009). Chemical studies of anthocyanins: a review. Food Chem. 113(4): 859-871. DOI: 10.1016/j.foodchem.2008.09.001

Chaves-Silva et al., 2018 – *Chaves-Silva S., Santos A.L., Júnior A., Zhao J.* (2018). Understanding the genetic regulation of anthocyanin biosynthesis in plants – Tools for breeding purple varieties of fruits and vegetables. *Phytochemistry,* 153: 11-27. DOI: 10.1016/j.phytochem.2018.05.013

Collard, Mackill, 2008 – *Collard B.C., Mackill D.J.* (2008). Marker-assisted selection: an approach for precision plant breeding in the twenty-first century. Philos. *Trans. R. Soc. Lond. B. Biol. Sci.,* 363(1491): 557-572. DOI: 10.1098/rstb.2007.2170

Damerum et al., 2015 – *Damerum A., Selmes S.L., Biggi G.F. et al.* (2015). Elucidating the genetic basis of antioxidant status in lettuce (Lactuca sativa). *Hortic. Res.,* 2: 15055. DOI: 10.1038/hortres.2015.55

Gazula et al., 2007 – *Gazula A., Scheerens J., Kleinhenz M.D., Ling P.* (2007). Anthocyanin Levels in Nine Lettuce (Lactuca sativa) Cultivars: Influence of Planting Date and Relations among Analytic, Instrumented, and Visual Assessments of Color. *HortScience*, 42(2): 232-238. DOI: 10.21273/HORTSCI.42.2.232

GBD 2017 Diet Collaborators, 2019 – GBD 2017 Diet Collaborators (2019). Health effects of dietary risks in 195 countries, 1990-2017: a systematic analysis for the Global Burden of Disease Study 2017. *Lancet*, 393(10184): 1958-1972. DOI: 10.1016/S0140-6736(19)30041-8

Gould, 2004 – *Gould K.S.* (2004). Nature's Swiss army knife: the diverse protective roles of anthocyanins in leaves. *J. Biomed. Biotech.* 5: 314-320. DOI: 10.1155/S1110724304406147

Guo et al., 2008 – *Guo J., Han W., Wang M.* (2008). Ultraviolet and environmental stresses involved in the induction and regulation of anthocyanin biosynthesis: A review. *Afr. J. Biotechnol.,* 7(25): 4966-4972.

Hansson et al., 2018 – *Hansson S.O., Åman P., Becker W. et al.* (2018). Breeding for public health: A strategy. *Trends Food Sci. Technol.,* 80: 131-140. DOI: 10.1016/j.tifs.2018.07.023

Khoo et al., 2017 – *Khoo H.E., Azlan A., Tang S.T., Lim S.M.* (2017). Anthocyanidins and anthocyanins: colored pigments as food, pharmaceutical ingredients, and the potential health benefits. *Food Nutr. Res.*, 61(1): 1361779. DOI: 10.1080/16546628.2017.1361779

Kitazaki et al., 2018 – *Kitazaki K., Fukushima A., Nakabayashi R. et al.* (2018). Metabolic Reprogramming in Leaf Lettuce Grown Under Different Light Quality and Intensity Conditions Using Narrow-Band LEDs. *Sci. Rep.,* 8: 7914. DOI: 10.1038/s41598-018-25686-0

Kwon et al., 2013 – *Kwon S., Simko I., Hellier B. et al.* (2013). Genome-wide association of 10 horticultural traits with expressed sequence tag-derived SNP markers in a collection of lettuce lines. *Crop J.*, 203; 1(1): 25-33. DOI: 10.1016/j.cj.2013.07.014

Lee et al., 2017 – *Lee Y.M., Yoon Y., Yoon H., Park H.M., Song S., Yeum K.J.* (2017). Dietary anthocyanins against obesity and inflammation. *Nutrients,* 9(10): E1089. DOI: 10.3390/nu9101089

Li et al., 2017 – *Li D., Wang P., Luo Y. et al.* (2017). Health benefits of anthocyanins and molecular mechanisms: Update from recent decade. *Crit. Rev. Food Sci. Nutr.*, 57(8): 1729-1741. DOI: 10.1080/10408398.2015.1030064

Liu et al., 2018 – *Liu Y., Tikunov Y., Schouten R.E. et al.* (2018). Anthocyanin biosynthesis and degradation mechanisms in Solanaceous vegetables: A review. *Front. Chem.*, 6: 52. DOI: 10.3389/fchem.2018.00052

Mampholo et al., 2016 – *Mampholo B.M., Maboko M.M., Soundy P., Sivakumar D.* (2016). Phytochemicals and Overall Quality of Leafy Lettuce (Lactuca sativa L.) Varieties Grown in Closed Hydroponic System. *J. Food Quality*, 39(6): 805-815. DOI: 10.1111/jfq.12234

Mouradov, Spangenberg, 2014 – *Mouradov A., Spangenberg G.* (2014). Flavonoids: a metabolic network mediating plants adaptation to their real estate. *Front Plant Sci.,* 5: 620. DOI: 10.3389/fpls.2014.00620

Mulabagal et al., 2010 – *Mulabagal V., Ngouajio M., Nair A. et al.* (2010). In vitro evaluation of red and green lettuce (Lactuca sativa) for functional food properties. *Food Chem.*, 118(2): 300-306. DOI: 10.1016/j.foodchem.2009.04.119

Nadeem et al., 2018 – *Nadeem M.A., Nawaz M.A., Shahid M.Q. et al.* (2018). DNA molecular markers in plant breeding: current status and recent advancements in genomic selection and genome editing. *Biothecnol. Biothecnol. Equip.,* 32(2): 261-285. DOI: 10.1080/13102818.2017.1400401

Pervaiz et al., 2017 – *Pervaiz T., Songtao J., Faghihi F. et al.* (2017). Naturally Occurring Anthocyanin, Structure, Functions and Biosynthetic Pathway in Fruit Plants. *J. Plant Biochem. Physiol.,* 5(2): 1000187. DOI: 10.4172/2329-9029.1000187

Provenzano et al., 2014 – *Provenzano S., Spelt C., Hosokawa S. et al.* (2014). Genetic control and evolution of anthocyanin methylation. *Plant Physiol.*, 165(3): 962-977. DOI: 10.1104/pp.113.234526

Rees et al., 2018 – *Rees A., Dodd G.F., Spencer J.P.E.* (2018). The effects of flavonoids on cardiovascular health: A review of human intervention trials and implications for cerebrovascular function. *Nutrients*, 10(12): E1852. Doi: 10.3390/nu10121852

Reis et al., 2016 – *Reis J.F., Monteiro V.V., de Souza Gomes R. et al.* (2016). Action mechanism and cardiovascular effect of anthocyanins: a systematic review of animal and human studies. *J Transl. Med.*, 14(1): 315. DOI: 10.1186/s12967-016-1076-5

Şakar et al., 2008 – *Şakar D., Karaoğlan G.K., Gümrükçü G., Özgür M.Ü.* (2008). Determination of Anthocyanins in some Vegetables and Fruits by Derivative Spectrophotometric Method. *Rev. Analyt. Chem.,* 27(4): 235-250. DOI: 10.1515/REVAC.2008.27.4.235

Santos-Buelga, González-Paramás, 2019 – *Santos-Buelga C., González-Paramás A.M.* (2019). Anthocyanins. Encyclopedia of Food Chemistry, pp. 10-21. DOI: 10.1016/B978-0-08-100596-5.21609-0

Smeriglio et al., 2016 – *Smeriglio, A., Barreca, D., Bellocco, E., Trombetta, D.* (2016). Chemistry, pharmacology and health benefits of Anthocyanins. *Phytother. Res.,* 30(8): 1265-1286. DOI: 10.1002/ptr.5642

Tanaka et al., 2008 – *Tanaka Y., Sasaki N., Ohmiya A.* (2008). Biosynthesis of plant pigments: anthocyanins, betalains and carotenoids. *Plant J.*, 54(4): 733-749. DOI: 10.1111/j.1365-313X.2008.03447.x

Volden et al., 2009 – *Volden J., Bengtsson G.B., Wicklund T.* (2009). Glucosinolates, l-ascorbic acid, total phenols, anthocyanins, antioxidant capacities and colour in cauliflower (Brassica oleracea L. ssp. botrytis); effects of long-term freezer storage. *Food Chem.,* 112(4): 967-976. DOI: 10.1016/j.foodchem.2008.07.018

Winkel-Shirley, 2001 – *Winkel-Shirley B.* (2001). Flavonoid biosynthesis. A colorful model for genetics, biochemistry, cell biology, and biotechnology. *Plant Physiol.,* 126(2): 485-493. DOI: 10.1104/pp.126.2.485

Yang et al., 2017 – *Yang L.P., Ling W.H., Du Z.C. et al.* (2017). Effects of Anthocyanins on Cardiometabolic Health: A Systematic Review and Meta-Analysis of Randomized Controlled Trials. *Adv. Nutr.* 8(5): 684-693. DOI: 10.3945/an.116.014852

Zhang et al., 2017 – *Zhang L., Su W., Tao R. et al.* (2017). RNA sequencing provides insights into the evolution of lettuce and the regulation of flavonoid biosynthesis. *Nat Commun.*, 8(1): 2264. DOI: 10.1038/s41467-017-02445-9